

VILNIUS UNIVERSITY
INSTITUTE OF BIOCHEMISTRY

Ilja Ignatjev

ESTERASE ACTIVITY DETECTION AT INTERFACES

Summary of doctoral dissertation
Physical sciences, biochemistry (04P)

Vilnius, 2009

The research was prepared at the Institute of Biochemistry in the period of 2004–2008.

Scientific supervisor:

doc. dr. **Gintaras Valinčius** (Institute of Biochemistry, physical sciences, biochemistry – 04 P)

The dissertation is defended at the Council of Biochemistry science direction of Vilnius University and Institute of Biochemistry:

Chairman:

prof. habil. dr. **Valdas Laurinavičius** (Institute of Biochemistry) (physical sciences, biochemistry 04 P)

Members:

prof. habil. dr. **Audrius Padarauskas** (Vilnius University, physical sciences, chemistry - 03 P)

prof. habil. dr. **Vida Mildažienė** (Vytautas Magnus University, physical sciences, biochemistry – 04 P)

dr. **Julija Razumienė** (Institute of Biochemistry, physical sciences, biochemistry – 04 P)

dr. **Evaldas Naujalis** (Semiconductor Physics Institute, physical sciences, chemistry – 03 P)

Opponents:

prof. habil. dr. **Albertas Malinauskas** (Institute of Chemistry, physical sciences, chemistry – 03 P)

dr. **Rolandas Meškys** (Institute of Biochemistry, physical sciences, biochemistry – 04 P)

The official discussion will be held on June 19, 2009 – 12 a.m. in the meeting of the Doctorate Committee at the hall of the Institute of Biochemistry.

Address: Mokslininkų 12, LT-08662 Vilnius, Lithuania.

The summary of the dissertation has been sent on May 19, 2009.

The dissertation is available at the library of the Institute of Biochemistry and at the library of Vilnius University.

VILNIAUS UNIVERSITETAS
BIOCHEMIJOS INSTITUTAS

Ilja Ignatjev

ESTERAZIŲ VEIKIMO FAZIŲ SĄLYČIO RIBOJE DETEKCIJA

Daktaro disertacijos santrauka
Fiziniai mokslai, biochemija (04 P)

Vilnius, 2009

Disertacija rengta 2004–2008 metais Biochemijos institute.

Mokslinis vadovas:

doc. dr. Gintaras Valinčius (Biochemijos institutas, fiziniai mokslai, biochemija – 04 P)

Disertacija ginama Vilniaus universiteto ir Biochemijos instituto biochemijos mokslo krypties taryboje:

Pirmininkas:

prof. habil. dr. **Valdas Laurinavičius** (Biochemijos institutas, fiziniai mokslai, biochemija – 04 P)

Nariai:

prof. habil. dr. **Audrius Padarauskas** (Vilniaus Universitetas, fiziniai mokslai, chemija - 03 P)

prof. habil. dr. **Vida Mildažienė** (Vytauto Didžiojo Universitetas, fiziniai mokslai, biochemija – 04 P)

dr. **Julija Razumienė** (Biochemijos institutas, fiziniai mokslai, biochemija – 04 P)

dr. **Evaldas Naujalis** (Puslaidininkų fizikos institutas, fiziniai mokslai, chemija – 03 P)

Oponentai:

prof. habil. dr. **Albertas Malinauskas** (Chemijos institutas, fiziniai mokslai, chemija - 03 P)

dr. **Rolandas Meškys** (Biochemijos institutas, fiziniai mokslai, biochemija – 04 P)

Disertacija bus ginama viešame biochemijos mokslo krypties tarybos posėdyje 2009 m. birželio 19 d. 12 val. Biochemijos instituto salėje.

Adresas: Mokslininkų 12, LT-08662 Vilnius, Lietuva.

Disertacijos santrauka išsiuntinėta 2009 m. gegužės. 19 d.

Disertaciją galima peržiūrėti Biochemijos instituto ir Vilniaus universiteto bibliotekose.

INTRODUCTION

Esterases belong to a large enzyme class that cleave ester bond of lipids at the oil/water interface. Enzymes investigated in the present work belong to the EC 3.1.1.x group in accordance to an international enzyme classification. Common feature of those enzymes is Ser–His–Asp(Glu) amino acid triad, in their active center. Esterases always were in the spotlight because their physiological importance and functional variability. Function of esterase depends on the source from which the enzymes were obtained. For example pancreatic lipases, are secreted into extracellular matrix where they hydrolyze dietary lipids into more simple compound forms, which can then be more easily absorbed and transported throughout the body. Meanwhile fungi and bacteria secrete esterases to facilitate nutrient absorption from the external medium. In humans lipases secreted from pancreas and liver play important role in food digestion, while phospholipases A₂ release arachidonic acid, a precursor of eicosanoids, paracrine hormones involved in reproductive function, wound or disease related pain and inflammation. Lipases are also relevant to many industrial applications. Lipases from microorganisms are used in detergents, oil and fat industries, baking, organic synthesis, hard surface cleaning, leather and paper industry, medicine (drugs production). Taking advantage of lipase property to distinguish between the optically active isomers, they are also used to separate them from the racemic mixtures.

Because of their physiological and technological importance understanding of mechanism of esterase activities is of utmost importance. To investigate/detect enzymatic activity/kinetics of esterases an appropriate water/oil interface must be utilized, which is usually prepared using various esters poorly soluble in water. Because of low solubility and in many cases amphiphilic nature of esters, the substrates may be present in different forms: monomers, micelles, monolayer films (at interface air/water), vesicles, bilayers, other aggregates or in a mixture of all those forms. However, enzymatic activity/kinetics strongly depends on of the particular form of a substrate. For example phospholipase A₂ is up to 1000 times more active on phospholipids aggregated in micelles compared to dissolved substrates. So it is of utmost importance, while analyzing enzymatic process, to utilize well-characterized and stable, time-independent substrate forms that would provide accurate data of enzyme activity.

Numerous methods are available for the detection and measuring hydrolytic activity of lipases: titrimetry, spectroscopy, fluorimetry, infrared spectroscopy, chromatography, turbidimetry, immunochemistry and other. Amongst them, the electrochemical-based assays exhibit advantage against others because of their applicability to heterogeneous, opaque systems. This feature of electrochemical techniques is extensively used in today's biosensor engineering. On the other hand, more and more spectroscopic techniques are developed, that allows detection of minute amount substances located at various interfaces. Our work was focused on developing new electrochemistry and spectroscopy methodologies to probe enzymatic activity of lipases. We sought to develop well-characterized heterogeneous substrates, which would be suitable for biosensor applications. In addition, new spectroscopy-based techniques, such as sum frequency generation spectroscopy was used to probe enzymatic activity of lipase at air/water interface thus providing proof-of-a-concept of the utility of SFG for bioanalytical applications. *Thermomyces lanuginosus* lipase and phospholipase A₂ were selected as model enzymes to accomplish tasks of this work. Practical significance of

these enzymes was the main reason of our choice. In addition, the choice of *Thermomyces lanuginosus* lipase (*TLL*) was partially related to the fact that the large portion of our work was an integral part of a FP6 “BIOSCOPE” project, in which *TLL* was one of the central enzymes project objectives were focused on.

The following objectives were pursued in this work:

- 1) Investigate the activity of *TLL* lipase by cyclic voltammetry using redox active ferrocene substrates physisorbed on solid surfaces.
- 2) To demonstrate the applicability of the rotating disk electrode technique to the detection of enzymatic activity of *TLL* using micellar redox active substrates.
- 3) To utilize physisorption effect of redox active synthetic naphthoquinone esters on glassy carbon electrodes from micellar solution to detect the *TLL* activity.
- 4) To demonstrate the applicability of Sum Frequency Generation spectroscopy to detect *TLL* activity at air/water interface.
- 5) To demonstrate the utility of tethered phospholipid bilayer membranes (tBLMs) as novel analytical platform to assay phospholipase A₂ and *TLL* activity by Electrochemical impedance spectroscopy (EIS).

The novelty and significance of the work

The activity is one of the major properties of enzymes providing information that allows investigating mechanisms of the enzymatic actions. In this work, we present several novel methodologies to assay enzymatic activities of esterases, in particular *TLL* and phospholipase A₂ that act at the boundaries between phases. In contrast to classical techniques that utilize micelle solutions of low solubility compounds, and therefore, often exhibiting polymorphism of the substrate, most of the methods described in this work are based on well-characterized and isomorphous substrates. This, we believe, could provide new experimental possibilities to investigating action mechanisms of enzymes such as *TLL* and PLA₂. The electrochemical and spectroscopic techniques described in this work may provide a new platform for various biosensor applications. On the other hand, to our best knowledge for the first time, we demonstrated the utility of non-linear spectroscopy methods to assay hydrolytic activity at air/water interface by lipases, and simultaneously demonstrating the capabilities of SFG spectroscopy to directly obtain molecular level information on both the enzyme and its substrate at the interface.

MATERIALS AND METHODS

Materials and sample preparation

Wild type (WT) *TLL* was obtained from Sigma (Germany); at concentration 34.5 mg/ml as measured by UV absorption at 280 nm). S146A mutant of *TLL* was provided by Novozymes A/S (Bagsvaerd, Denmark) in a form of 3-6 mg/ml solution. The purity of the enzyme was checked by SDS-PAGE, about 10 % of enzyme was denaturated, that's why before measurements lipase was cleaned using 14 kDa dialysis membrane. Synthesis of all substrates except phospholipids was accomplished at the Institute of Biochemistry in Bioelectrochemistry and Biospectroscopy department. 1,2-dioleoyl-*sn*-glycero-3-phosphocholine (DOPC) and 1-palmitoyl-2-oleoyl-*sn*-glycero-3-phosphocholine (POPC) were used as supplied from Avanti Polar Lipids (Birmingham, AL, USA). All buffer solutions were prepared using ultrapure water from a Millipore Milli-Q PF plus reagent grade water purification system.

Cyclic voltamperometry measurements

The solid-supported substrates for cyclic voltammetry were made using commercially available polycrystalline gold electrodes (Bionalytical Systems, Inc., West Lafayette, IN) which were polished on 0.05 μm alumina slurry (Struers, Denmark) and sonicated for 5-10 min. in a 1:1 mixture of water and ethanol solution. The surface of gold electrodes was functionalized by either self assembled monolayer (SAM) of 9-Mercaptononyl-5'-ferrocenylpentanoate (MNFcP) or some redox-inactive alkanethiol or its derivative. In most parts of the work 1 mM 1-hexanethiol (HT) was used. The functionalization was carried out by 3 hour incubation in an ethanol (95%) solution of 1 mM MNFcP or ethanol (95%) solution of alkanethiol as 1 mM 1-hexanethiol (HT). In case of the redox-inactive SAM, atop of it, a layer of synthetic enzyme substrate containing ferrocene and ester groups (9-(5'-ferrocenylpentanoyloxy)nonyl disulfide (FPONDS), decanoyl-5'-ferrocenylpentanoate (DFcP), 9-bromnonyl-5'-ferrocenylpentanoate (BrNFcP), 9-mercaptononyl-5'-ferrocenylpentanoate (MNFcP), (\pm)9-mercaptononyl-3-methyl-5'-ferrocenylpentanoate (MNMFP)) was deposited via a simple "drip-and-dry" procedure. Specifically, the first step gives the chemically anchored 1HT-SAM, which shields the underlying metal surface from direct contact with the substrates and later, with the protein molecules. Next, a fixed volume droplet of 25 μM substrate solution in ethanol (95%) is placed atop the gold-supported 1HT-SAM, and the solvent is allowed to evaporate. The solution spread over the whole electrode plane, including the metal and the insulating resin parts. The concentration and the volume of the ethanol solution is chosen such that, after evaporation, the effective surface concentration of the electroactive substrate is close to the packing density of one monomolecular layer of ferrocene. The overlayer of deposited electroactive molecules is stable in aqueous buffer solutions for prolonged periods of time, however, the stability varied between different substrates. Cyclic voltammetry measurements were carried out on a VersaStat (EG&G) computerized potentiostat system (Princeton Applied Research, Princeton, USA) using three electrode conventional electrochemical setup. Platinum wire was used as the auxiliary electrode and saturated sodium calomel electrode (SSCE) was used as the reference. The real surface area of the working electrode was estimated from

the integration of Au surface oxidation charge between 0.9 and 1.45 V in 0.1 M sulfuric acid solution. It was estimated as $(4.50 \pm 0.05) \cdot 10^{-2} \text{ cm}^2$ on 0.02 cm^2 geometric surface electrodes. All measurements were carried out at room temperature at $20 \pm 2 \text{ }^\circ\text{C}$ unless otherwise indicated.

Rotation Disc Electrode (RDE) measurements

RDE-2 rotating disk electrode (RDE) unit (Bioanalytical systems, Inc., West Lafayette, IN, USA) was used throughout the work. A glassy carbon working electrode MF-2066, platinum coil auxiliary electrode MW-1033 and Ag/AgCl reference in 3 M NaCl MF-2052 (all from Bioanalytical Systems, Inc., West Lafayette, IN, USA). In this part of the work, the potentials are referred to this reference electrode. The electrode rotation speed was set to 100 rpm. Each time before recording the voltammogram, the surface of the working electrode was briefly (0.5–1 min) polished on a polishing cloth using $0.05 \text{ }\mu\text{m}$ alumina slurry (Struers, Denmark). The measurement of enzymatic activity was carried out as follows. $50 \text{ }\mu\text{l}$ of Triton X-100 was added to a 19.95 ml solution of 0.01 M phosphate buffer (pH 7.0), containing 0.1 M NaCl (solution 1). In a separate vial, the lipase target solution (solution 2) was prepared by dissolving 2 mg of O-palmitoyl-2,3-dicyanohydroquinone (PDCHQ) or 2.1 mg 2-OxyPalmitoyl-1,4-NaphthoQuinone (OPNQ) in 1 ml of 96% ethanol at $40 \text{ }^\circ\text{C}$. The solutions were left to equilibrate at $40 \text{ }^\circ\text{C}$ in a thermostated bath for about 10 min. Then, 9 ml of solution 1 was transferred to the electrochemical cell thermostated at $40 \text{ }^\circ\text{C}$, to which subsequently 1 ml of solution 2 was added. Immediately after the mixing of solutions 1 and 2, the background (PDCHQ case) or initial (OPNQ case) voltammogram was recorded. After the addition of enzyme, the electrochemical response was monitored in the potential range from 0 to 0.7 V (PDCHQ case) or from 0 to -1.0 V (OPNQ case) by applying linear potential scan at the rate of 20 mV/s . To relate the magnitude of the limiting current I_{lim} of the RDE and concentration of the enzymatically generated 2,3-dicyanohydroquinone, we used the Levich equation. To analyzing OPNQ hydrolysis rate Levich and adsorption kinetics formalism were utilized.

Electrochemical impedance spectroscopy (EIS) measurements

EIS measurements were performed using a Princeton Applied Research Parstat 2273 (EG&G, USA) electrochemical workstation. To analyze EIS data ZView (Scribner Associates, USA) equivalent circuit modeling software was used. Spectra were obtained at frequencies between 0.5 and 65000 Hz with ten logarithmically distributed measurements per decade. They are presented in Cole-Cole plots ($\text{Im } C$ vs $\text{Re } C$, where $C=C(\omega)$ is the frequency-dependent capacitance of the electrode and ω is the angular frequency, $\omega = 2\pi f$, with f the frequency in Hz. Gold-coated silicon wafers ($20 \times 40 \text{ mm}^2$) served as the working electrode in a setup that allowed simultaneous EIS measurements in six electrochemical cells (volume $V = 220\text{--}240 \text{ }\mu\text{l}$) on each wafer. The geometric surface areas of gold exposed to the solution was $S_{\text{mean}} = 0.34 \pm 0.02 \text{ cm}^2$. while the roughness factor β , estimated from the gold surface oxidation/oxide stripping charge, was between 1.7 and 1.9 for different samples. A saturated silver-silver chloride $\text{Ag}|\text{AgCl}|\text{NaCl}_{(\text{aq},\text{sat})}$ microelectrode model M-401F (Microelectrodes, Bedford, NH, USA) was used as reference. The auxiliary electrode was a 0.25 mm diameter platinum

wire (99.99% purity, Aldrich, USA) coiled around the barrel of the reference electrode. The distance between the tip of the reference and working gold electrode surface was set to 2–3 mm. All measurements were carried out at 0 V bias versus the reference electrode at room temperature (20 ± 2 °C) in aerated solutions.

A 1-thiahexa(ethylene oxide) lipid, 20-tetradecyloxy-3,6,9,12,15,18,22-heptaohexatricontane-1-thiol (WC14), was donated by Dr. David J. Vanderah (National Institute of Standards and Technology, Gaithersburg, MD, USA).

WC14 SAMs serving as molecular anchors of phospholipid bilayer were prepared by incubating freshly magnetron-sputtered gold wafers in ethanolic solution of WC14 and β -mercaptoethanol (β -ME) at molar ratios WC14: β -ME 3:7, and total concentration of thiolated compounds 0.2 mM. The wafers were incubated for 3-4 h. After removal of the samples from the incubation solutions they were rinsed with absolute ethanol and dried in a nitrogen stream. Once coated with a SAM, the substrates could be stored for up to one week and used after rinsing with ethanol to prepare tethered bilayer membranes (tBLMs). The protocol of preparation was as follows. A 10 mM solution of lipid in absolute ethanol was allowed to incubate the SAM-covered substrate for 5 min at room temperature. It was then rapidly (within 10–15 s) displaced by a large excess of aqueous buffer solution, taking care to avoid the formation of air bubbles at the surface that could disturb the SAM. Typically, a 45 μ l droplet of the phospholipid solution was vigorously flushed with 10 ml of buffer. The buffer used was either 10 mM Tris-HCl (tris(hydroxymethyl) aminomethane-HCl) or 10 mM phosphate buffers, pH 7.3-9.3, containing Na^+ salts (0.1–0.2 M) with 1 mM EDTA (to bind Ca^{2+}). All exchanges were performed at 20 ± 2 °C.

Surface Plasmon resonance (SPR) measurements

The SPR measurements were carried out on GES-5 type spectral ellipsometer (SOPRA, France) containing a 75 W collimated xenon lamp as the light source, a polarizer, and a high refraction index 60° SF10 glass prism, the base of which was covered by thermally evaporated about 50 nm thick gold film. An 1-octadecanethiol (ODT) layer was chemically deposited by incubating prism in 0.2 mM ethanol solution of ODT. The base of the prism, together with the gold film and ODT layer, was immobilized in a special cell filled with a phosphate buffer solution (0.01 M NaH_2PO_4 and 0.1 M NaCl adjusted to pH 7.0 with NaOH). The SPR cell was arranged in a way that allowed injection of *TLL* into the chamber so that the interaction of ODT SAM with enzyme was possible to monitor in real time. The SPR spectral measurements were carried out in collaboration with dr. Z. Balevičius (Institute of Physics, Vilnius), who carried out the analysis and modeling of the SPR signal.

Attenuated total reflection Fourier-transform infrared (ATR-FT-IR) spectroscopy measurements

ATR-FT-IR is widely used by researchers to examine a variety of sample types including solids, powders, pastes and liquids for food analysis, biomedical applications, polymers, and thin films. In addition to the identification of functional groups during more routine analysis, ATR-FT-IR spectroscopy is useful for mechanistic studies of

vapor-solid interactions during chemical vapor deposition or heterogeneous catalysis by *in situ* real time monitoring of surface species ATR-FT-IR spectra were recorded with the same Perkin-Elmer Model Spectrum GX FT-IR spectrometer equipped with DGTS (deuterated triglycine sulfate) detector. The spectral resolution was set to 4 cm^{-1} , and all of the spectra were acquired by 500 scans.

The flowing cell for ATR-FT-IR measurements was made in our laboratory from teflon. In the teflon basement was insert o-ring with 0.32 cm^2 area, which is correspond to area of the working electrode surface. This cell was attached to ZnSe prism. Into collected cell was injected $10\text{ }\mu\text{L}$ of $25\text{ }\mu\text{M}$ 1,16-di-(5'-ferrocenylpentanoyloxy) hexadecane (**FPOHD**) and drying with Ar gas. In the following way the physisorbed substrate monolayer was prepared onto ZnSe surface.

The amide I vibrational region (1642 cm^{-1}) of FT-IR spectra was fitted by Gaussian components, number and position of which were determined from the second derivatives of the experimental profile. The peak positions of the components were allowed to vary within 2 cm^{-1} from initial values during fitting procedure. Fitting was performed with Gaussian functions by using GRAMS AI software assuming linear baseline line. ATR-FT-IR measurements were carried out by D. Milkantaite, and the spectral data analysis was carried out in collaboration with dr. G. Niaura.

Surface-enhanced infrared absorption (SEIRA) spectroscopy measurements

For the SEIRA spectroscopy experiments, the chemically deposited gold films were prepared as follows. Polished $0.3\text{--}0.4\text{ mm}$ thick silicon ($15\times 15\text{ mm}$ samples) wafers were immersed for 10 min in a 10% $(\text{NH}_4)_2\text{S}_2\text{O}_8$ solution in concentrated sulfuric acid. Then, the electrodes were washed with copious amounts of MilliporeTM deionized water. The wafers were transferred to a 40% water solution of NH_4F for 3 min, to dissolve the SiO_2 layer from the surface, dried in a stream of argon, and then put onto the metallic plate thermostated at $60\text{ }^\circ\text{C}$. For the gold plating, we premixed $60\text{ }\mu\text{l}$ of gold plating solution HAuCl_4 with $120\text{ }\mu\text{l}$ of 2% HF solution, and the whole liquid amount was allowed to spread onto the freshly NH_4F -pretreated silicon wafer surface to obtain a gold film $\sim 1.2\text{--}1.5\text{ cm}^2$ in area. After $60\text{--}90\text{ s}$, the process was stopped by intense rinsing with room temperature deionized water. Then, gold coated wafer was rinsed with 95% ethanol and immediately transferred to a solution of 1 HT (1 mM) for 3 h for SAM formation. SEIRA measurements were performed on Perkin-Elmer, model Spectrum GX FT-IR spectrometer equipped with DGTS detector. The spectral resolution was set at 4 cm^{-1} , and all of the spectra were acquired by 500 scans. Buffers were made using ASC reagent grade sodium salts and sodium hydroxide purchased from Sigma-Aldrich Chemie GmbH. The buffer containing 0.1 M NaClO_4 , 0.01 M monobasic sodium phosphate, adjusted with NaOH to pH 7.0 was used for SEIRA experiments.

Sum frequency spectroscopy (SFG) measurements

SF spectra were recorded using EKSPLA (Vilnius, Lithuania) picosecond SFG spectrometer. The spectrometer is based on a mode-locked EKSPLA PL2143A/20 Nd:YAG laser generating 28 ps pulses at 1064 nm with 20 Hz repetition rate. In some experiments, EKSPLA PL2143A/50 Nd:YAG laser-generating pulses with 50 Hz

repetition rate was employed. The second harmonic radiation (wavelength 532 nm, pulse energy 300-400 μJ) from this laser was used as a visible beam (ω_{VIS}). The tunable infrared pulses (ω_{IR}) in the 1500–3750 cm^{-1} frequency region with the energies of 80–200 μJ were produced in parametric generator EKSPLA PG401VIR/DFG pumped by third harmonic (355 nm) and fundamental radiation of the laser. The bandwidth of ω_{IR} was $< 6 \text{ cm}^{-1}$. To produce SFG spectra, the ω_{IR} and ω_{VIS} beams were incident at angles of 53 and 60°, respectively, and overlapped at the sample within an area of 0,04 mm^2 . The sum frequency (ω_{SF}) radiation was filtered by holographic notch filter and monochromator and detected by a photomultiplier tube and gated registration system. Typically, the signal was averaged over 100 pulses. However, in time-resolved experiments 60 pulses were co-added. On an average, the noise in these experiments was $\sim 12\%$ of the signal intensity. SFG spectra were normalized according to intensity of infrared beam to take into account the changes in ω_{IR} energy with wavelength. The frequencies were calibrated by IR spectrum of polystyrene film placed in the path of the infrared beam. Two modes of SFG data acquiring were used. First, SFG spectra were collected by scanning of IR beam wavelength, and second SFG dynamics was observed by registering SFG signal changes in time at particular wavelength. To extract the parameters of SFG resonances, the experimental spectra have been fitted using eq 1

$$I_{\text{SDG}} = \left| \chi_{\text{NR}}^{(2)} + \sum \frac{A_n e^{i\psi_n}}{\omega_{\text{IR}} - \omega_n + i\Gamma_n} \right|^2 \quad (1)$$

where I_{SFG} is the sum frequency intensity, $\chi_{\text{NR}}^{(2)}$ is the nonresonant contribution to the nonlinear susceptibility, and A_n , ψ_n , ω_n , and Γ_n are the strength, relative phase, resonant frequency, and line width of the n th vibration, respectively. SFG experiments were conducted in a cylindrical glass cell, which was 38 mm in diameter. Before experiments, the cell was cleaned first with sodium hydroxide solution and subsequently with a mixture of concentrated nitric and sulfuric acid solutions. After these procedures, the cell was washed with ultrapure (Millipore purified) water. The cleanness of the cell and studied aqueous phase was checked by SFG spectroscopy. No peaks in the C-H stretching region were detected before spreading the PDCHQ, which indicated absence of organic contaminants at studied solution/air interface. SFG measurements were repeated 3–5 times by using newly prepared similar samples. The experiments were carried out at room ($\sim 20 \text{ }^\circ\text{C}$) temperature.

The SFG experiments were carried out in collaboration with dr. G. Niaura and dr. Z. Kuprionis (EKSPLA, Vilnius), while the spectral data analysis and interpretation was done by dr. G. Niaura.

RESULTS AND DISSCUSION

Cyclic voltammetry detection of *TLL* activity using redox active substrates physisorbed on solid surfaces

The main idea based on which the method described in this section works is as follows. The conducting surface is functionalized with the synthetic compound contains two functional groups: the ester and ferrocene moieties. The ester group serves as a target for the bond cleaving enzyme, e.g., esterase. The ferrocene redox group acts as a

reporter, which generates the electrochemical signal detectable by the cyclic voltammetry. Because the bond cleavage results in the formation of water-soluble ferrocene derivative (in our case ferrocene pentanoic acid), one may expect that esterase activity will be monitored by the decay of a redox signal.

The functionalization of the gold surface by the thiolated compounds is well-studied technique yielding, in most cases, durable and reproducible organic self-assembled monolayers. Therefore, we first attempted to utilize MNFcP (thiol group-terminated compound containing ester bond, see cartoon in Fig. 2) SAMs to monitor enzymatic activity of esterases. We expected that chemically attached to the surface molecules will provide robust bioanalytical platform for the detection of the activity of ester bond-cleaving enzymes, such as *TLL*. Cyclic voltammetry curves are shown in Fig. 2.

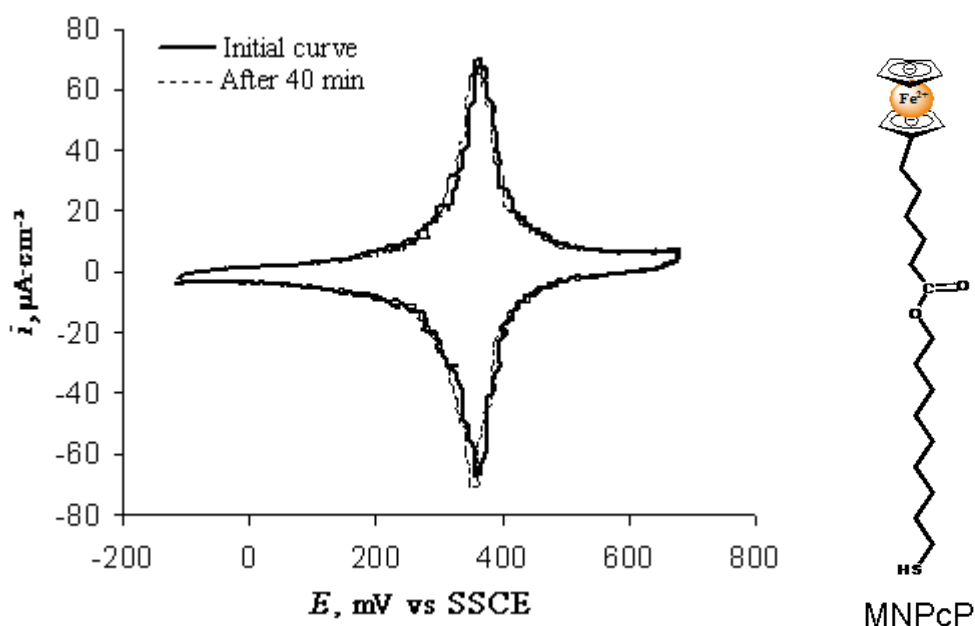


Fig. 2. Cyclic voltammetry curves of MNFcP SAM on Au electrode before and after incubation (time = 40 min) with *TLL*. Concentrations: 25 μM *TLL*, 0.1 M NaClO_4 and 0.01 M Na_2HPO_4 buffer solution, pH 7, at room temperature. Potential scan rate, $V_E = 100$ mV/s, initial surface density of ferrocene reporting groups $\Gamma_{\text{MNFcP}} = 4.5 \cdot 10^{-10}$ mol/cm².

However, as we can see, there are no significant changes in the electrochemical signal of the SAM after incubation with the lipase for 40 min. Obviously, we encounter either inactivity of the enzyme towards chemically linked to the solid surface MNFcP molecules or inability of released ferrocenylpentanoic acid to leave the surface upon cleavage. Further experimental data suggested that the enzyme most likely experienced difficulties in accessing the target ester group in a relatively densely packed SAM of MNFcP. Therefore, instead of using compounds that are chemically linked to the gold, we applied different strategy of planting substrate onto the electrode surface. As described in Materials and methods section, we put a droplet of ethanol solution of ferrocene terminated disulfide FPONDS compound (see cartoon in Figure 3) onto the HT-thiol protected gold electrode and let the droplet to dry out. We expected that in such

way deposited disulfide will form physisorbed layer, in which FPONDS molecules will be less constrained, thus allowing esterase active center to effectively bind target group and cleave the ester bond.

The experimental data in Figure 3 demonstrates that, indeed, FPONDS molecules are not forming chemical bonds with gold surface, and can be easily removed from the surface by dissolution in ethanol. The ferrocene oxidation-reduction current maxima seen in CV (Fig. 3, B) after the FPONDS layer is formed on HT-modified gold surface (Fig. 3, A) by “drip-and-dry” method almost totally disappear after 5 min of immersion in 95% ethanol (Fig. 3, C).

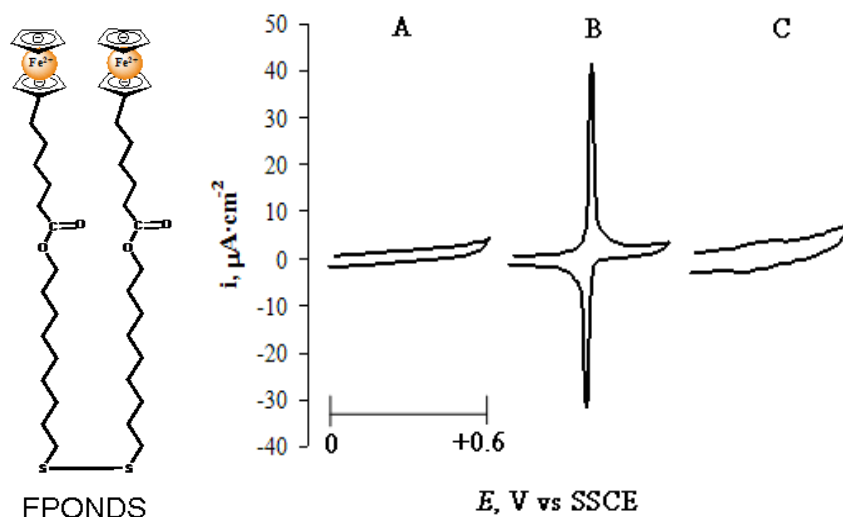


Fig. 3. Cyclic voltammetry (CV) curves obtained at different stages of lipase target layer formation/destruction. (A) CV signal from the gold surface covered by HT SAM, (B) FPONDS layer formed by spreading 5 μl droplet of a 25 μM FPONDS solution onto the surface (C) same as in (B) “drip-and-dry” FPONDS layer after 5 min of immersion in 95% ethanol. Curve B is four times reduced for better comparison with A and C curves. The potentials are plotted with respect to the saturated sodium calomel electrode. Potential scan rate = 100 mV/s. Estimated electrode surface = 0.04 cm^2 .

This indicates that the drip-and-dry FPONDS layer, otherwise stable to aqueous buffers (vide infra), is unstable in ethanol (removal of essentially all FPONDS molecules). In our opinion, this is a direct proof of the physisorbed state of the FPONDS molecules on the substrate surface. Otherwise, if the FPONDS would be able to form sulfur-gold bond during the course of drying of the FPONDS solution, one would not expect the removal of chemically bound thiolate by a short time incubation in ethanol. In our opinion, these facts support the assumption that the drip-and-dry FPONDS overlayer is not linked to the surface via chemical bonds.

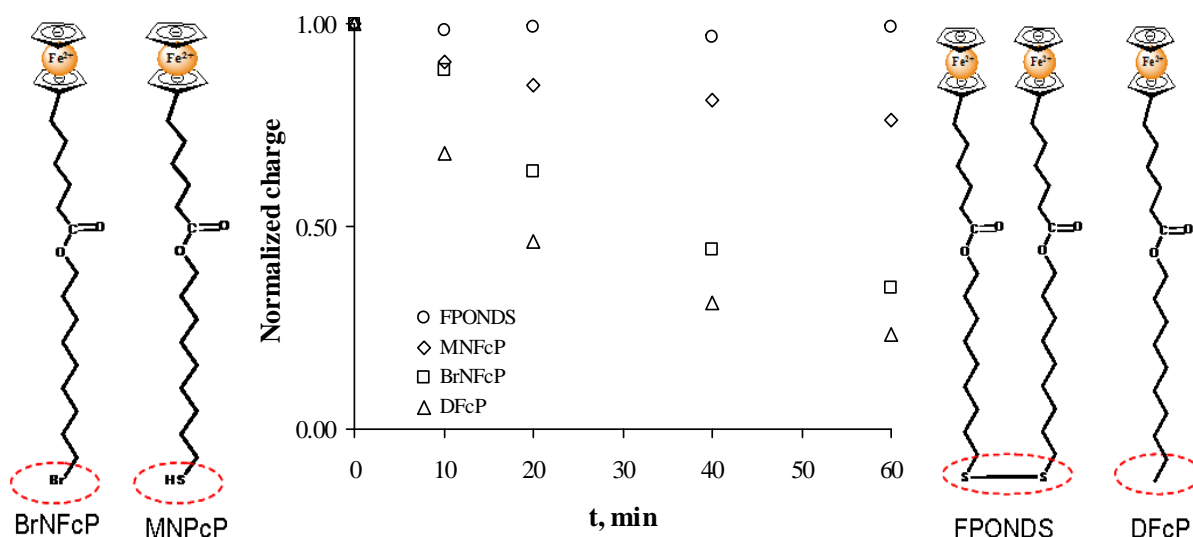


Fig. 4. Normalized integrated charge vs time of drip-and-dry layer incubation in 0.1 M NaCl, 0.01 M phosphate buffer at pH 7.0 at room temperature. All other electrochemical parameters are the same as in Figure 2. Abbreviations: 9-Bromononyl-5'-ferrocenylpentanoate (BrNFcP), decyl-5'-ferrocenylpentanoate (DFcP), 9-mercaptononyl-5'-ferrocenylpentanoate (MNFcP), and 9-(5'-ferrocenylpentanoyloxy)nonyl disulfide (FPONDS).

Figure 4 demonstrates the stability of FPONDS and other related compounds to 60 minute exposure to the unstirred phosphate buffer solution at pH 7.0. This data demonstrate that the terminus group of the hydrocarbon chain strongly affects the stability of the physisorbed ferrocene compound. Obviously, FPONDS, which is the largest molecule, forms most stable in aqueous environment. This justifies the choice of FPONDS as a substrate for further analysis of the hydrolysis process triggered by *TLL*.

The initial curve in Figure 5 shows the voltammetric redox response of the electrode due to the presence of the ferrocene group in the FPONDS molecules on the surface. Without external polarization, the response was stable for at least 1 h in a quiescent buffer solution (Fig. 4) However, moderate agitation of the solution with a magnetic stirrer bar (~100 rpm) results in a slight decay of the initial signal at a rate of less than 0.2%/min.

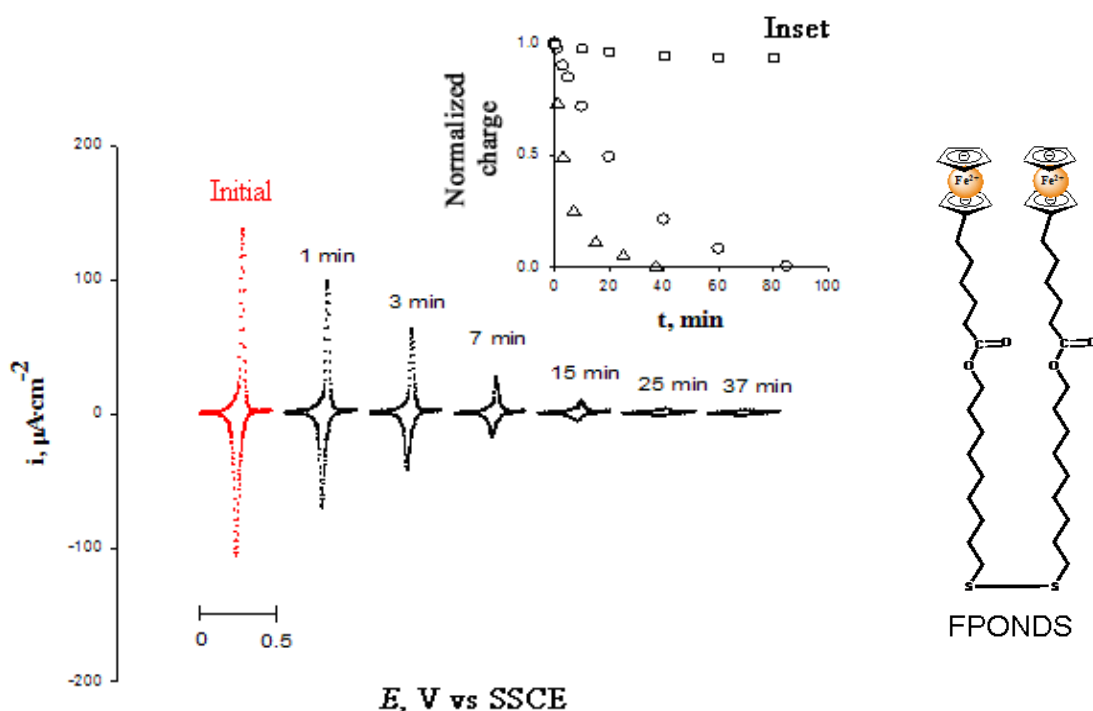


Fig. 5. Cyclic voltammetry curves of FPONDS-based substrate upon addition of *TLL* in the amount of $C(TLL) = 2.5 \mu\text{M}$ in 2 ml of buffer solution. The numbers next to the curves indicate the time (min) elapsed after the addition of *TLL*. All curves recorded at 100 mV/s scan rate, in the potential interval from 0 to 0.5 V vs SSCE. Buffer composition: 0.1 M NaClO_4 , 0.01 M phosphate buffer, pH 7.0, 25 °C. Initial surface concentration of FPONDS: $2.7 \cdot 10^{-10} \text{ mol}/\text{cm}^2$ on surface. Estimated surface area of the gold electrode: 0.042 cm^2 .

Inset: decay of the normalized integrated peak current of the electrode in the quiescent solutions at various lipase concentration: 0 (squares), 0.25 μM (circles), and 2.5 μM (triangles) in 2 ml of buffer solution.

On the other hand, under continuous potential cycling, in the interval from 0 to 0.5 V (vs saturated sodium chloride calomel electrode; SSCE), the decay rate of the initial voltammetric signal becomes noticeable even in the quiescent solution. Under such conditions, typical rate of decay was $\sim 0.4\%/ \text{cycle}$. Noteworthy, when calculating initial rates of interfacial enzymatic reactions, small spontaneous deterioration of the signal (usually below 2–3%) generally results in insignificant errors. Upon lipase addition (Figure 5), changes in the cyclic voltammetry curve are clearly seen, which can be assigned to the *TLL* activity. The peak current, which magnitude is proportional to the number of ferrocene groups in the surface layer, decreases upon lipase injection. As can be seen from the inset of Figure 5, the rate of decrease of the peak current integral is proportional to the amount of injected enzyme. This suggests that the rate of electrochemical signal decay can be used to determine the *TLL* activity. Although the decrease of the redox response is due to changes in the ferrocene groups at the surface, it is not clear from these data alone that the current decrease is due to the hydrolytic cleavage of the ester bond by *TLL*. In principle, there could be other reasons for the disappearance of signal. For example, the protein might compete with the FPONDS molecules for surface adsorption sites. To demonstrate that the ester bond is specifically

cleaved by the lipase, we recorded the SEIRA spectra (Figure 6) of the substrate exposed to the *TLL* solution.

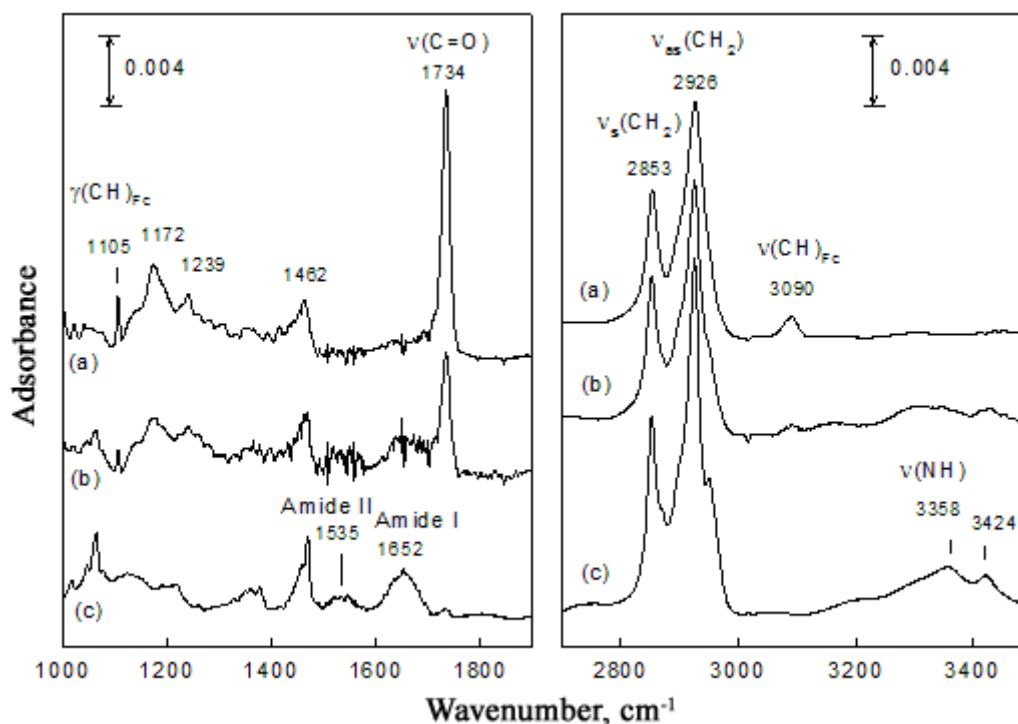


Fig. 6. SEIRA spectra of the FPONDS/HT/Au/Si substrate in the middle- and high-frequency regions measured after different times of incubation in the quiescent *TLL*-containing solution: (a) 0, (b) 1, and (c) 15 h. The background spectrum of the HT/Au/Si substrate was subtracted. A total of 500 scans at 4 cm^{-1} resolution were accumulated. Incubation solution: 4 ml of 0.1 M NaClO_4 , 0.01 M phosphate buffer of pH 7.0, containing $5\text{ }\mu\text{M}$ of *TLL*. Initial amount of FPONDS is $\sim 1.7 \cdot 10^{-9}\text{ mol/cm}^2$.

The SEIRA signal was measured in a transmission mode using chemically deposited Au films on silicon. To increase the sensitivity, we first recorded the spectrum of the gold surface modified by 1 HT-SAM. Then, the FPONDS overlayer was deposited, and the sum spectrum of the physisorbed FPONDS and 1HT-SAM was recorded. The difference of these two spectra, which is shown in Figure 6 a, is the pure spectrum of FPONDS. In the middle frequency domain (Figure 6 a, left graph), the narrow out-of-plane ferrocene ring vibrational band at 1105 cm^{-1} , and strong ester carbonyl band at 1734 cm^{-1} are clearly seen. In the high-frequency range (Figure 6 a, right graph), the CH stretching vibrational band of the ferrocene ring at 3090 cm^{-1} and a family of the symmetric and antisymmetric CH stretching vibrational bands of the alkyl chain at 2853 and 2926 cm^{-1} , respectively, are evident. The peak positions of CH modes are sensitive to the order of the polymethylene chain. The frequencies in Figure 6 are higher by several reciprocal centimeters as compared with the well-ordered crystalline-like structures (2850 and $2917\text{--}2920\text{ cm}^{-1}$), indicating that the polymethylene chains of physisorbed FPONDS are disordered, containing a number of gauche defects. Upon addition of *TLL*, the SEIRA spectrum starts to change. Spectrum b in Figure 6 shows the SEIRA signal obtained after 1 h of incubation of the substrate in the unstirred enzyme solution.

The first and the most important observation is that the decrease in the intensities of the ferrocene and carbonyl group bands occurs simultaneously. After 1 h of *TLL* exposure, the integrated spectral intensities of these two bands decrease to ~40% from the initial values. After 15 h of incubation in the lipase solution, both bands exhibit about the same residual integrated intensity level of ~3%. On the other hand, incubation in the *TLL* solution for 1 h induces only slight perturbations on the intensities of CH vibrational bands (e.g., the integrated intensity of the 2853 cm⁻¹ band decreases from 0.29 to 0.26), indicating that the main polymethylene chain of FPONDS remains on the surface. This supports the assumption that the removal of the ferrocene moieties from the surface occurs primarily via the cleavage of ester bond.

Another important result is seen in Figure 6 b. The amide I and amide II bands at 1652 and 1535 cm⁻¹ (Figure 6 b, left graph) as well as the NH stretching vibrational band at 3358 cm⁻¹ (Figure 6 b, right graph) appear upon exposing the substrate wafer to the lipase solution. These bands indicate protein anchoring to the surface, which is known to be a necessary step for the initiation of *TLL* enzymatic action. These spectral changes continue to increase with substrate/*TLL* solution contact time. The ferrocene bands totally disappear (Figure 6 c), concurrent with the reduction of the much stronger carbonyl band at 1734 cm⁻¹ to barely above the spectral baseline level. The integral intensity of this spectral line is less than 3% of the initial value. Thus, enzyme-induced cleavage of the ester bond proceeds until the substrate material is almost completely consumed. On the other hand, the protein bands (1535, 1652, and 3358 cm⁻¹) continue to increase relative to the 1 h spectrum (Figure 6 b). This suggests that the kinetics of the enzyme action might be determined by the protein adsorption/anchoring rate in unstirred solutions. Even though Figure 6 presents clear evidence that the ester bond is cleaved upon injection of *TLL*, the SEIRA data alone do not yield direct prove that the bond rupture occurs through an enzymatic mechanism. To confirm the enzymatic nature of the ester bond hydrolysis, the following experiment was performed

It is known that the catalytic triad of amino acids Ser-His-Asp determines the hydrolytic activity of *TLL* with the Ser146 acting as a nucleophile. Along with the wild type (WT) *TLL*, we applied a mutant variant of the enzyme, in which Ser146 in the catalytic triad was substituted with alanine (S146A mutant of *TLL*). Compared to the WT enzyme, the S146A protein exhibits ~500 times lower hydrolytic activity. Thus, within the time frame used in the cyclic voltammetry measurement of the initial hydrolysis rate of FPONDS molecules (≤ 10 min), there is virtually zero activity for this variant of *TLL*.

Figure 7 compares the voltammetric responses in the presence of WT and mutant lipases. It is evident (Figure 7, filled circles) that the S146A mutant does not induce changes in the voltammetric signal. Within 60 min after the mutant injection, the integral of the peak current decreases by $\leq 4-5\%$, which is comparable to natural deterioration rate of the FPONDS layer (vide ultra).

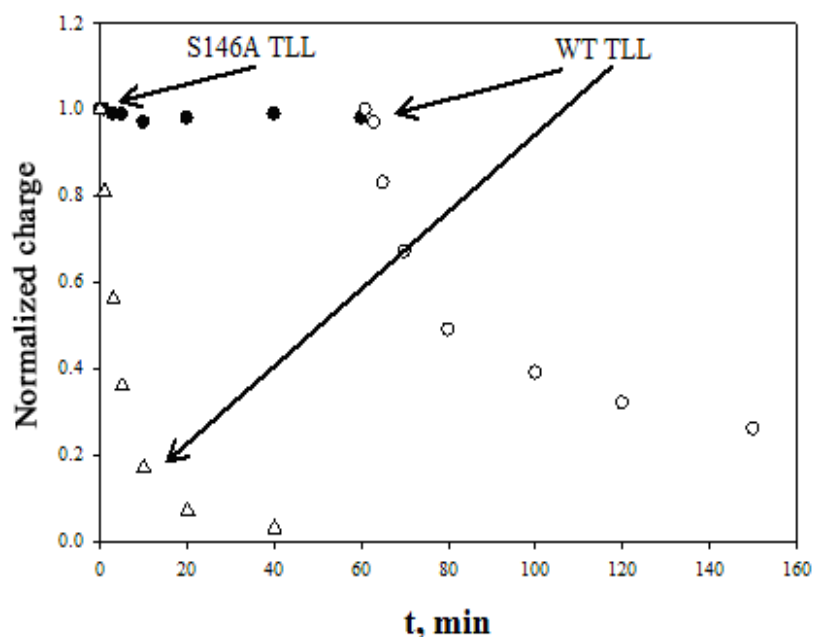


Fig. 7. Normalized integrated voltammetric peak of the FPONDS/HT/Au substrate vs time of the electrode incubation in the quiescent solutions containing WT *TLL* or S146A mutant *TLL* plus WT *TLL*. Concentrations of the WT *TLL* (triangles and open circles) and S146A mutant *TLL* (filled circles) in the solutions: 3.5 and 9.25 $\mu\text{g/ml}$, respectively. In 2 ml of solution containing 0.1 M NaClO_4 , 0.01 M phosphate buffer of pH 7.0, 25 $^\circ\text{C}$. Initial surface concentration of FPONDS is $\sim 2.6 \cdot 10^{-10}$ mol/cm², estimated surface area of the gold electrode: 0.042 cm².

However, once the native lipase is injected, the integrated voltammetric signal immediately starts to decay (Figure 7, open circles). Figure 7 reveals one more interesting detail. The rate of signal decay is clearly dependent on whether the buffer contains an inactive mutant before the injection of WT enzyme. The electrochemical signal decays much slower (in Figure 7, ~ 5 times) if the mutant enzyme is present in the system prior to the WT enzyme injection. We believe, this result is consistent with the idea that, being present in the solution, both active and inactive proteins compete for the surface. It is widely acknowledged that in order to cleave the ester bonds the lipase molecule must anchor itself to the hydrophobic substrate surface. Hence, when the mutant the S146A is present in the solution prior to injection of the WT enzyme, the inactive competitor occupies part of the substrate's surface.

Therefore, the reduced hydrolysis rate (Figure 7, compare open circles and triangles) testifies that the cleavage of the ester bond of FPONDS occurs via an enzymatic mechanism.

Since the enzymatic reaction occurs at the interface to estimate the hydrolysis turnover rate the surface concentration of the enzyme is required. To make these estimates we referred to the SPR and IR spectroscopy techniques. The experimental data is summarized in Figure 8. To simulate the hydrophobic, though enzymatically non-active, substrate surface we utilized ODT monolayer on gold. Upon injection of the lipase, we observed a shift in the plasmon resonance minimum, which let us make estimates of the thickness and the refractive index of an organic layer that is formed on the surface (Figure 8 a).

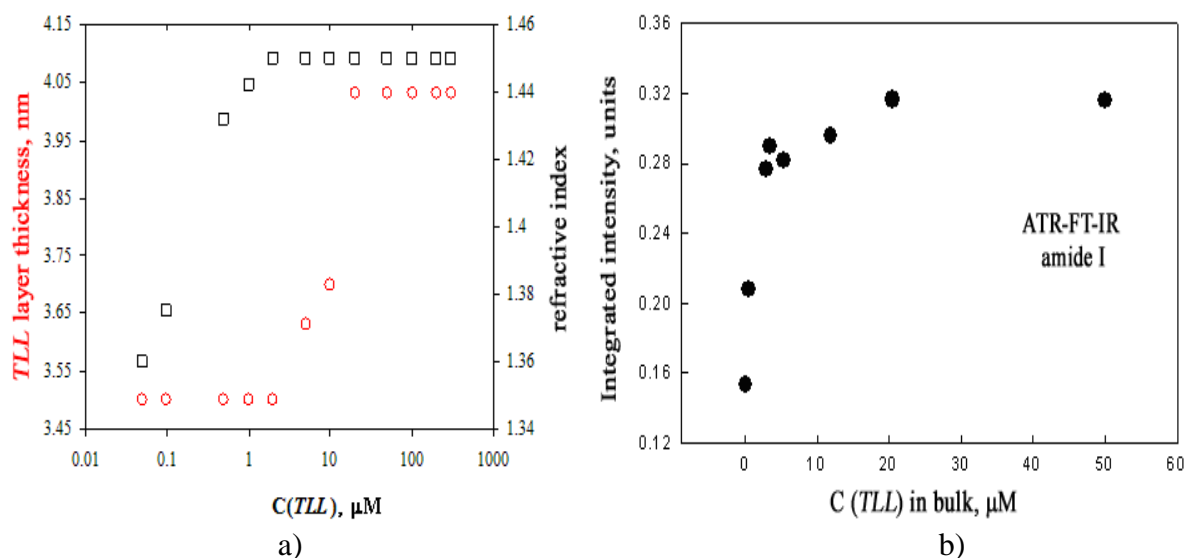


Fig. 8. Observation of *TLL* adsorption by: a) SPR and b) ATR-FT-IR methods.
 a) *TLL* adsorption layer thickness on 1 ODT SAM (\circ) and refractive index (\square) dependence of *TLL* concentration in the bulk, b) Changes of integrated amide I peak intensity of FPOHD physisorbed monolayer on ZnSe. upon addition *TLL* into the solution. Buffer: 0.1 M NaCl in 0.01 M NaH_2PO_4 , pH 7; $T = 20^\circ\text{C}$.

It is seen from Figure 8 a that the refractive index of the organic layer that is building up upon *TLL* injection increases from 1.352 to 1.450 as the concentration of the protein changes from 0.05 to $2\ \mu\text{M}$. Interestingly, in the same concentration range SPR spectra modeling indicates no effective thickness changes. Such feature suggests that in this concentration range the enzyme molecules may be continuously filling up the surface adsorption sites, while the effective layer thickness remains constant and equals to 3.5 nm. This number is comparable to a molecular height of *TLL* laying flat on a surface. At higher concentrations ($>2\ \mu\text{M}$), the refractive index reaches maximum available value of 1.450. However, as the variation of the refractive index halts the effective thickness of the layer starts increasing and at about $20\ \mu\text{M}$ of *TLL* saturates at 4.05 nm. This suggests the compacting of the adsorption layer, and possibly the change in protein molecule orientation from flat to vertical

This conclusion is strongly supported by the ATR-FT-IR spectroscopy data (Figure 8 b), which indicates rapid increase of the integral intensity of an Amide I vibration band in the protein concentration range from 0.05 to $\sim 2\ \mu\text{M}$. At higher concentrations the growth of Amide I band slows down, and almost saturates at $\sim 20\ \mu\text{M}$. So, assuming the vertical position of adsorbed *TLL* molecule on the surface, and taking into account the physical size of *TLL*, we estimate maximal adsorbed quantity of *TLL* on the hydrophobic model surface to be $\sim 3.9 \cdot 10^{-7}\ \text{g}/\text{cm}^2$. This number allows us to determine the absolute enzymatic activity of *TLL* on FPONDS substrate (see dissertation for details). The summarized data in Table 1 present clear evidence of a sharp acceleration of an enzymatic action as the concentration of *TLL* reaches $2.5\ \mu\text{M}$. This is a threshold beyond which SPR spectroscopy data shows the saturation of the refractive index and start of the effective layer increase. These experimental observations support the hypothesis according to which at this *TLL* concentration the reorientation of enzyme molecules on the surface starts occurring.

Table 1: Absolute *Thermomyces lanuginosus* lipase activity on FPONDS. in 0.01 M phosphate buffer (pH 7.0, at room temperature), containing 0.1 M NaClO₄ determined from integrated FPONDS peak current decrease from 0.13 V to 0.5 V (vs saturated sodium chloride calomel electrode) in time. Real surface area of the electrode: 0.042 cm².

1	2	3	4	5
Concentration of TLL in buffer, μM	Surface amount of TLL, $\times 10^8$ g	Amount of FPONDS on the surface, $\times 10^{11}$ mol	Specific enzyme activity, $\mu\text{mol}/(\text{min g})$	Amount of FPONDS hydrolysed by one TLL molecule per minute, 1/min
0.025	0.75	1.90 \pm 0.15	60 \pm 5	1.75 \pm 0.15
0.25	1.06	2.40 \pm 0.40	80 \pm 15	2.35 \pm 0.45
2.5	1.37	2.00 \pm 0.15	530 \pm 40	15.55 \pm 1.17

We may conclude that in order to achieve a significant enzymatic activity two conditions must be met i) a certain degree of disorder and mobility inside the aggregated substrate layer, and ii) saturation of the substrate surface by the enzyme to the level at which the TLL molecules are forced to accept inclined position. On the other hand, the degree of freedom cannot exceed a threshold beyond which the substrate systems unstable. Such molecules as MNFcP, BrNFcP and DFcP, were found to form unstable overlayers, therefore less suitable for enzymatic activity detection. It is conceivable that the methodology we developed to detect enzymatic activity of TLL, or simple modifications thereof, could be used for other bond-cleaving enzymes.

Electrochemical assay for lipase detection using micellar substrate system

It is well known that the electrochemical analytical techniques are practically insensitive to the presence of solid or/and liquid light scattering microparticles in the solutions, so they provide means for the detection of enzyme activity in opaque samples. The electrochemistry instrumentation could be also easily designed in the form of portable devices. This prompted us to develop a novel electrochemical lipase activity assay based on the amperometric detection of the hydrolysis product. The principle of the assay is as follows. A lipid-like synthetic compound *O*-palmitoyl-2,3-dicyanohydroquinone (PDCHQ)¹ that contains both the ester and the electroactive hydroquinone-based groups served as a lipase substrate. PDCHQ molecules are solubilized in the form of the Triton X-100 micelles, while the product of enzymatic hydrolysis, 2,3-dicyanohydroquinone, is soluble in water so it could be readily oxidized on the electrode in a diffusion-controlled process. Under the diffusion control, the

¹ The structure of PDCHQ is shown on p. 29 of this Summary.

magnitude of the electrode current is determined solely by the concentration and diffusion coefficient of the electroactive species (in our case, 2,3-dicyanohydroquinone) and the effective thickness of the diffusion layer. The latter could be easily controlled using forced convection electrochemical techniques, such as rotating disk electrode voltammetry. Consequently, the diffusion-limiting current of 2,3-dicyanohydroquinone oxidation can be utilized for the assay of lipase activity.

Typical experimental voltammograms are shown in Figure 9. The initial current–potential curve of a freshly prepared PDCHQ solution exhibits virtually no electrochemical response in the potential range from 0 to 0.7 V. This means that, in this potential range, the lipase micellar substrate PDCHQ is electrochemically inactive.

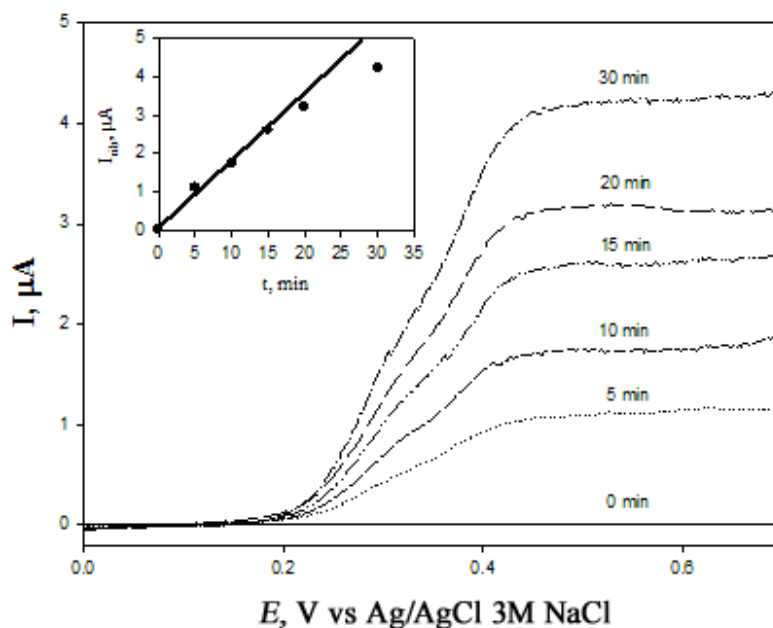


Fig. 9. Background-subtracted voltammograms of 0.5 mM *O*-palmitoyl-2,3-dicyanohydroquinone (PDCHQ) in 10 ml of 0.01 M phosphate buffer (pH 7.0, 40 °C), containing 0.1 M NaCl and 0.25 vol. % Triton X-100, at the glassy carbon rotating (100 rpm) disk electrode (0.07 cm² area, potential scan rate 20 mV/s) before (0 min) and after (5, 10, 15, 20, and 30 min) addition of a 200 μl aliquot (6.90 mg protein) of *Thermomyces lanuginosus* lipase. The inset shows the limiting current value at the potential 0.5 V as a function of enzyme action time. In the inset, the initial rate of current increase (182 nA/min) is indicated by the solid line. For the spontaneous nonenzymatic hydrolysis, this slope equals ca. 2 nA/min (not shown).

Upon injecting lipase, a current wave develops at $E \geq 0.2$ V, which corresponds to the oxidation of 2,3-dicyanohydroquinone, as determined by replacing PDCHQ with 2,3-dicyanohydroquinone in the solution. The electrochemical response, generated by lipase, exhibits current plateau, which magnitude linearly increases with the square root of the RDE rotation speed (not shown). This suggests the diffusion-controlled nature of the limiting current. As seen from Figure. 9, the limiting current plateau increases with time thus allowing assessment of the initial rate of the enzymatic process (see the inset of Fig. 9, constructed using the current values at 0.5 V). To relate the magnitude of the limiting current I_{lim} of the RDE and concentration of the enzymatically generated 2,3-dicyanohydroquinone, we used the Levich equation (2):

$$I_{\text{lim}} = 0.62nFAD^{2/3}\omega^{1/2}\nu^{-1/6}C^* \quad (2)$$

where $n = 2$ is the number of electrons participating in the overall electron transfer reaction, $F = 96485 \text{ C/mol}$ is the Faraday number, $A = 0.07 \text{ cm}^2$ is the surface area of the working electrode, $D = 5.49 \cdot 10^{-6} \text{ cm}^2/\text{s}$ is the diffusion coefficient of 2,3-dicyanohydroquinone (obtained in a separate RDE experiment from the I_{lim} vs $\omega^{1/2}$ plot), $\omega = 10.5 \text{ s}^{-1}$ is the angular frequency of rotation, $\nu = 0.01 \text{ cm}^2/\text{s}$ is the kinematic viscosity for dilute aqueous solutions, and C^* is the bulk concentration (mol/cm^3) of the electroactive substance.

Table 2 summarizes the hydrolysis rates recorded on the RDE as a function of the volume of the lipase aliquots injected.

Table 2: *Thermomyces lanuginosus* lipase activity with respect to *O*-palmitoyl-2,3-dicyanohydroquinone in 0.01 M phosphate buffer (pH 7.0, 40 °C), containing 0.1 M NaCl and 0.25 vol. % Triton X-100, determined at 0.5 V (vs Ag/AgCl, 3 M NaCl) using the glassy carbon rotating (100 rpm) disk electrode of 0.07 cm² area

1	2	3	4	5	6
Enzyme solution aliquot, μl	Protein amount, mg	Current increase rate due to spontaneous hydrolysis, nA/min	Total current increase rate, nA/min	Activity $\times 10^3$, $\mu\text{mol}/\text{min}$	Specific activity, $\mu\text{mol}/(\text{min g})$
100	3.45	~2	93±3	50.67	14.69
200	6.9		182±14	100.22	14.52
300	10.5		276±23	152.56	14.53
Mean:					14.58±0.11

The fourth column of the table contains the electrochemical data, which are obtained by (i) measuring the initial rate of limiting current increase in the presence of lipase and (ii) subtracting the rate of limiting current increase due to the spontaneous hydrolysis of PDCHQ (third column). The latter was approximately 2 nA/min. The fifth column data are obtained using the Levich equation, while the sixth column is a result the division of the activity data by the protein amount (second column). As expected, the initial rate of I_{lim} increase is proportional to the amount of lipase added to the solution. This result confirms the possibility of monitoring lipolytic activity by using the technique of amperometric detection (for the continuous monitoring, in the chronoamperometric mode at constant electrode potential) and by applying the synthetic substrates containing electrochemically active hydrolysis product. For the *TLL*, the mean value of specific

activity obtained equals ca. 14 $\mu\text{mol}/(\text{min g})$ (Table 2), and it is about 40 times lower than the parameter determined in the parallel spectrophotometric *para*-nitrophenyl palmitate - based assay (measurements were performed by adapting the substrate preparation method described by Gupta et. al.² to the conditions of our amperometric assay; the experimentally determined molar extinction coefficient of *para*-nitrophenyl palmitate at 400 nm and pH 7.0 was $6900 \text{ M}^{-1}\cdot\text{cm}^{-1}$).

Lower specific activity, however, does not significantly influence the quality of the assay because the interfering rate of spontaneous hydrolysis (expressed in electrochemical units) of ca. 2 nA/min is relatively low compared to the enzymatic hydrolysis rate (Table 2). On the other hand, the origin of such a significant distinction between the specific activities calls for further investigations.

Detection of enzyme activity utilizing the electrochemical response of adsorbed substrate

A common problem in detection enzymatic activity of esterases is a polymorphism of substrates that typically are poorly soluble in water esters. Dispersed in aqueous medium substrate molecules may aggregate in different forms, such as micelles, insoluble aggregates, precipitates, adsorbed layers, etc. Once the enzyme is introduced into the system, and the enzymatic cleavage starts, the rate of the hydrolysis product release could be used as a measure of the enzyme activity. Unfortunately, in case of the polymorphous substrates, the product release occurs from the different substrate forms simultaneously. Such a drawback is especially undesirable in research model systems, in which the precise characterization of the experimental conditions is a must. On the other hand, micellar systems are relatively easy to prepare and handle. This prompted us to develop the enzyme activity detection technique, which would be free from aforementioned shortcomings, and at the same time would take advantage of the simplicity of the preparation of micellar systems.

The method described below is based on the phenomenon that was discovered by us in the course of this work. Specifically, knowing the propensity of quinone and naphthoquinone compounds to form adsorbed layers on graphite (glassy carbon) surfaces, we tested the ability of poorly soluble naphthoquinone esters to form similar layers from the solutions, in which naphthoquinone-containing molecules are predominantly located in the micelles. We expected that micelles upon interaction with the graphite surface would be able to donate naphthoquinone-containing molecules, which being transferred to the surface may form adsorbed monolayer. If so, then it should be possible to electrochemically detect the presence of the naphthoquinone derivative by using cyclic voltammetry. For such an experiment we chose 2-Oxypalmitoyl-1,4-Naphthoquinone (OPNQ), micelles, which were prepared in a similar fashion as PDCHQ micelles described in the previous chapter. Indeed, the micelles generated the reversible electrochemical response, which indicted the establishment of the equilibrium between the OPCQ molecules in the micelles and the surface.

² N. Gupta, P. Rathi, R. Gupta, Simplified *para*-nitrophenyl palmitate assay for lipases and esterases, *Anal. Biochem.* **2002**, 311, 98–99.

Typical current-potential curve of a freshly prepared glassy carbon electrode in OPNQ micelle solution is shown in Figure 10 (red curve). The curve exhibits three distinct regions: a maximum around -0.2 V, a low plateau between -0.3 V and -0.6 V, and high plateau beyond -0.7 V. The maximum at around -0.2 V is independent on RDE rotation speed, however, it is dependent on the concentration of OPNQ micelle in bulk. It also scales linearly with potential scan rate, which indicates the adsorptive nature of the current peak. Conversely, the current plateau beyond -0.7 V is dependent on the square root of RDE, which is indicative of the diffusion control of the electrochemical process that takes place in this potential range. The current in the intermediate range from -0.3 V and -0.6 V has a complex nature that is discussed more thoroughly in the dissertation.

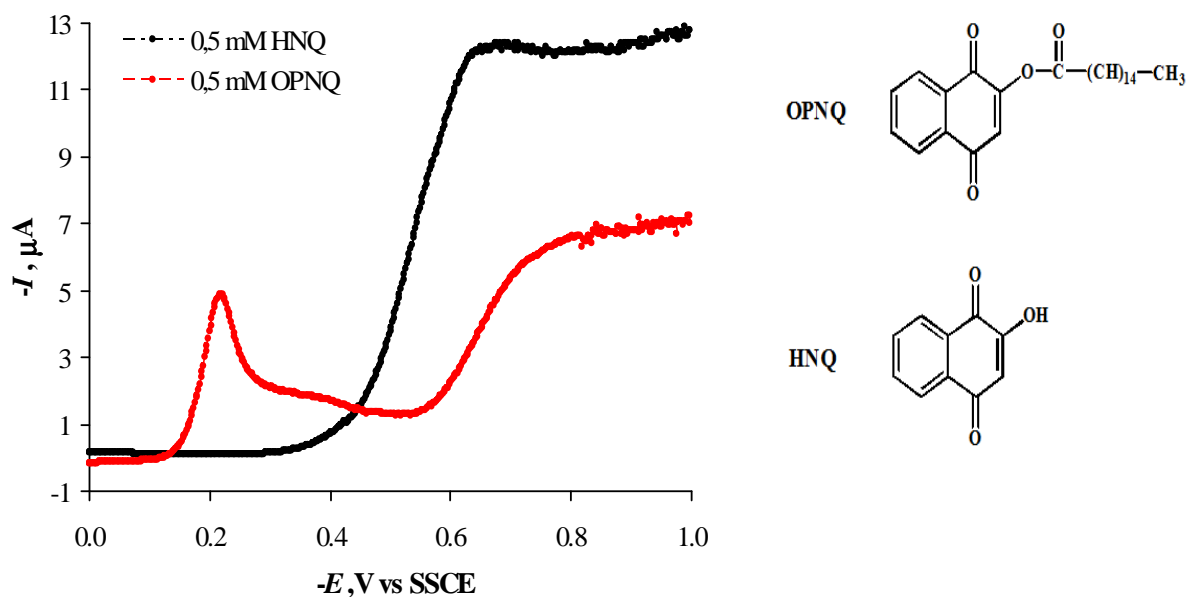


Fig. 10. Background-subtracted voltammograms of 0.5 mM 2-Oxypalmitoyl-1,4-Naphthoquinone (OPNQ) and 2-Hydroxyl-1,4-Naphthoquinone (HNQ) in 10 ml of 0.01 M phosphate buffer (pH 7.0, 40 °C), containing 0.1 M NaCl and 0.25 vol. % Triton X-100, at the glassy carbon rotating (100 rpm) disk electrode (0.07 cm² area, potential scan rate 20 mV/s).

The dependence of the height of the current peak at -0.2 V from concentration of OPNQ suggests that it could be utilized to detect the micelle concentration in the solution, and consequently, to track the enzymatic activity of the esterases such as *TLL*. Integrated between the potentials from 0.0 and 0.33 V current values are plotted in Figure 11 as a function of OPNQ concentration. It is evident, that the plot presented in the inverted Langmuir coordinates confirms that the equilibrium between the OPNQ concentration in the solution and surface amount of reducible OPNQ is of adsorptive nature, and is a measure of the concentration of OPNQ micelles. Thus, the enzymatic activity could be measured by the rate of the electrochemical signal decrease upon the injection of an esterase into the solution. As seen from Figure 10 (black curve), the released OPNQ hydrolysis product HNQ is not electrochemically active in the potential range from 0 and -0.33 V, therefore it is not interfering with the electrochemical signal of OPNQ.

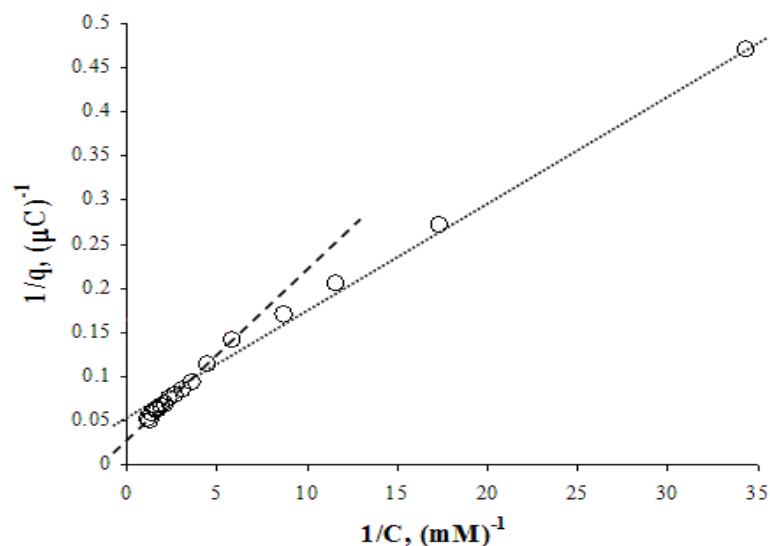


Fig. 11. OPNQ reduction charge dependence from OPNQ concentration in inverted Langmuir isotherm coordinates. All measurements carried out under aerobic conditions. Buffer: 0.1 M NaCl in 0.01 M NaH₂PO₄, pH 7, C(Tritono X-100) = 0.25%, $V_E = 20$ mV/s, $\omega = 100$ rpm, $T = 40$ °C, $S_{\text{geometric}} = 7.06 \cdot 10^{-2}$ cm².

The summary of the *TLL* activity data obtained by integrated current measurements and by the classical spectroscopic assay is compared in Table 3. Obviously, qualitatively similar results are obtained by using two different techniques. One may expect that in case same substrates are used in both assays the detected enzyme activities must exhibit similar values. Indeed, this is the case, as it is seen from the data in Table 3.

Table 3. *Thermomyces lanuginosus* specific enzyme activity detected at various pH values by the electrochemical and spectroscopic methods.

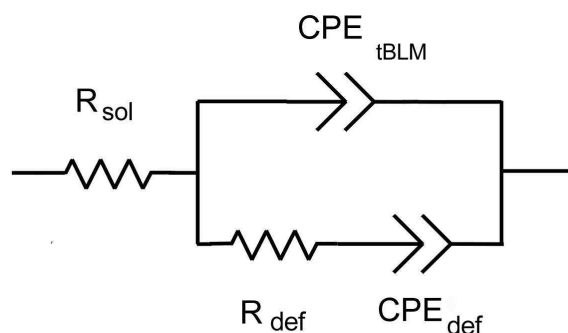
pH	Specific activity detected using spectroscopy method, $\mu\text{mol}/(\text{min} \cdot \text{g})$	Specific activity detected using electrochemistry method, $\mu\text{mol}/(\text{min} \cdot \text{g})$
7	70 ± 5	40 ± 5
7.8	90 ± 5	50 ± 5
8.7	170 ± 5	155 ± 5
9.6	150 ± 5	115 ± 10

However, it is also obvious that the electrochemical technique indicates consistently lower measured activities in comparison to the spectrophotometric assay. The observed difference could be explained by taking into account the fact that in the spectrophotometric experiments the rate of enzymatic process is measured by the amount of the released product, and the latter could be released from any form of the substrate material present in the system. However, in the electrochemistry experiments, the rate of enzyme reaction is followed by amount of only one, micellar, form of the substrate remaining at certain moment of time in the system, even though the substrate is a polymorphous system. Interestingly, at higher pH the difference between the data obtained by different techniques tends to decrease. This most likely could be explained by the fact that at higher pH the solubilization of amphiphilic OPNQ occurs more easily,

rendering more homogeneous substrate composition. We, therefore, conclude that the electrochemical method described in this work may be used to detect the esterase activity by using the physisorption equilibrium established between the micelles and the surface of the glassy carbon electrodes.

Electrochemical impedance spectroscopy (EIS) in enzyme activity detection using tethered bilayer membranes

Tethered bilayer membranes are novel surface supported model systems that mimic natural bilayers. Recently, the utility of the tBLMs for the enzymatic activity assay of the phospholipase A₂ (PLA₂) has been demonstrated.³ In this work, we further developed the method by extending some of the technical capabilities of the proposed methodology. The main instrumental technique, which is used in this work, is an Electrochemical Impedance Spectroscopy (EIS). It was shown⁴ that the response of the tBLMs both in the presence and absence of the enzymes (proteins) may be modeled by the electric equivalent model shown in Scheme 1, while for the monitoring phospholipase A₂ action the variation of the total frequency dependent electrode capacitance (measured at fixed modulation frequency) was suggested.



Scheme 1. Electric equivalent model of the EIS response of tBLMs. R_s – is the solution resistance, CPE_{tBLM} – is the constant phase element, which models the capacitance of the membrane, R_{def} and CPE_{def} – are correspondingly the resistance and constant phase element reflecting the conductance pathway of naturally occurring or artificially introduced defects.

However, since the electrode capacitance measured at one single frequency has contributions from different physical phenomenon occurring at the interface, it is more rational to follow individual elements of the electric equivalent to detect interaction between the enzymes and the membrane. The EIS spectral analysis carried out in accordance to the model in Scheme 1 yields values of R_{def} and CPE_{tBLM} , both of which respond to phospholipase A₂ once the co-factor Ca^{2+} is added to the system (Figure 12)

³ G. Valincius, D. J. McGillivray, W. Febo-Ayala, D. J. Vanderah, J. J. Kasianowicz, M. Losche. *J. Phys. Chem. B.*, **2006**, 110, 10213–10216.

⁴ D. J. McGillivray, G. Valincius, D. J. Vanderah, W. Febo-Ayala, T. J. Woodward, F. Heinrich, J. J. Kasianowicz, M. Losche. *Biointerphases*. **2007**, 2, 21-32.

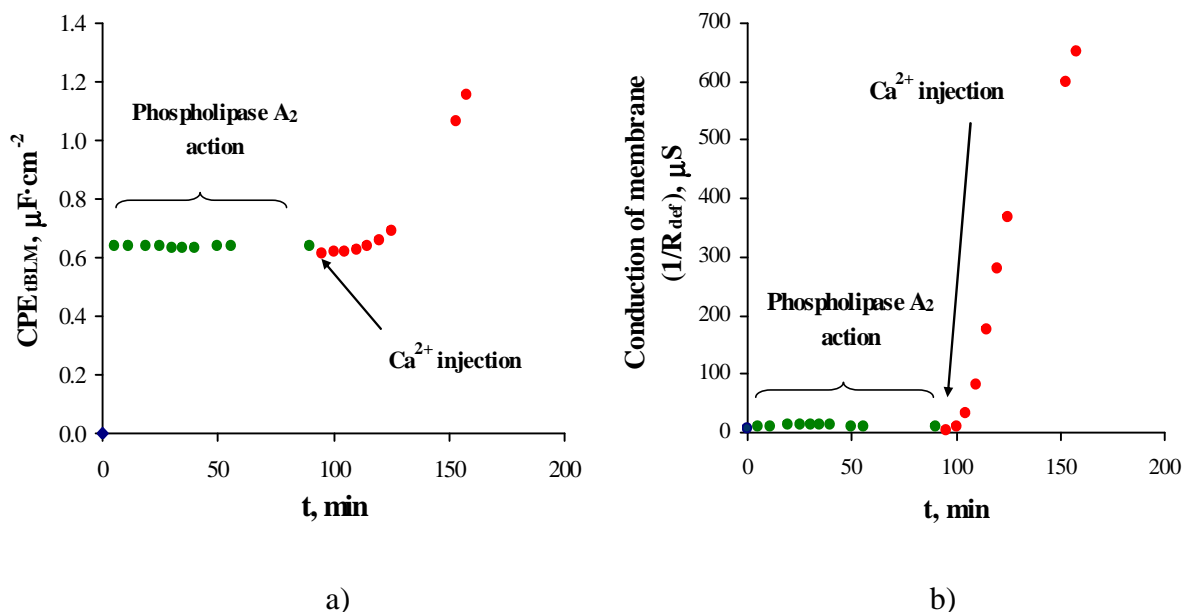


Fig. 12. Variation of CPE_{tBLM} and $1/R_{def}$ upon injection of phospholipase A₂ in POPC tBLM system. Results get from EIS spectra, using fitting equivalent model. $C(PLA_2_{pp}) = 300$ nM, $C(Ca^{2+}) = 2$ mM. Buffer: 0.01 M TRIS, 1 mM EDTA, 0.1 M NaCl, pH 7.3, $T = 22 \pm 3$ °C, $S_{electrode} = 0.45$ cm².

The time-profile of the reaction is consistent with the enzymatic nature of observed changes of R_{def} and CPE_{tBLM} . After the addition of phospholipase A₂ into the electrochemical cell, the membrane parameters remain stable for at least 2 hours (green part of the curves, Figure 12). However, once the Ca²⁺ is added, both parameters start changing in a way consistent with an enzymatic digestion of the phospholipid bilayer by phospholipase A₂. The CPE_{tBLM} and $1/R_{def}$ (the ohmic conductance associated with the defects) starts increasing. In addition, as it might be seen from the comparison of Figures 12 a and 12 b, one could expect that the sensitivity of the phospholipase activity detection will be much greater in $1/R_{def}$ case the slope of the $1/R_{def}$ curve is many times higher compared to the capacitance curve. To test the applicability of the observed parameter changes for enzymatic activity detection, we carried out a series of EIS measurements at different PLA₂ concentrations. The data is summarized in Figure 13. First, it is obvious that POPC membranes are significantly more susceptible to PLA₂ action, in comparison to the DOPC membranes. Second, in both cases, one may observe a correlation between the initial $1/R_{def}$ increase rate and enzyme concentrations, which is almost linear in case of DOPC, while there is noticeable deviation from linearity in case of POPC.

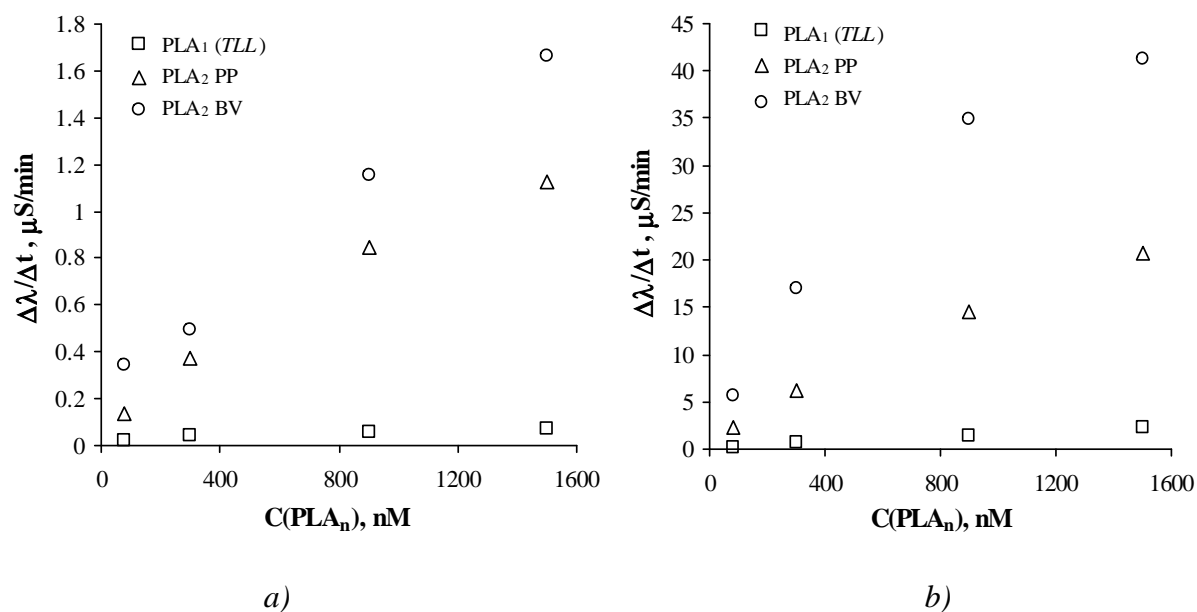


Fig. 13. Membranes formed from different phospholipids hydrolysis rate when in system where are various phospholipases A₂ (with cofactor $C(\text{Ca}^{2+}) = 2 \text{ mM}$) and phospholipases A₁ (TLL) concentrations. Buffer: 0.01 M TRIS, 0.1 M NaCl, 1 mM EDTA, Ph 7.3, $T = 22 \pm 3 \text{ }^\circ\text{C}$, $S_{\text{electrode}} = 0.45 \text{ cm}^2$. Membrane type: a) DOPC tBLM, b) POPC tBLM

Another interesting feature of the curves in Figure 13 is clear distinction between esterases: TLL does not exhibit hydrolysis action on both types of tBLMs. While the PLA₂ from bee venom is generating consistently stronger response in both DOPC and POPC systems compared to PLA₂ from porcine pancreas.

The results reported here thus show that EIS-based technique in combination with tBLMs can be a useful tool for both esterase activity detection in phospholipid systems and characterization of membranes of different compositions. This has practical significance. Because the enzymatic activity is concentration dependent, tBLM-based devices can be developed to monitor for secretory PLA₂.

Detection of lipase activity at air/water interface by Sum-Frequency Generation (SFG) spectroscopy

To understand and control biocatalytic processes at surfaces, detailed molecular level information on organization of interface is required. Most of the traditional methods for investigation of air/liquid interface yield macro-level physical and chemical information or lack required molecular sensitivity. Among the experimental techniques suitable for such studies, vibrational sum-frequency generation (SFG) spectroscopy seems particularly attractive, because of molecular specificity and intrinsic interfacial sensitivity. In this work, the application of SFG spectroscopy for monitoring enzymatic process at air/water interface is described. As in previous chapters, for the prove-of-a-concept purpose TLL was chosen. As mentioned earlier, a challenging problem in elucidating the catalytic mechanism of lipases, in general, and TLL, in particular, is related to the polymorphism and complexity of organizational state of aggregated

substrates (e.g. triglycerides), which, under the experimental conditions, is difficult to control. From this perspective, SFG vibrational spectroscopy may offer an alternative that allows to avoid aforementioned difficulties because the recorded enzyme activity signal, in this case, is generated only by the organized asymmetric surface layer of substrate and enzyme at air-water interface. Therefore, the main objective of the current chapter was to directly detect enzymatic activity of a lipase (*TLL*) and to characterize the molecular environment of the interphase, in which the hydrolysis takes place. For this purpose, we used custom synthesized substrate O-palmitoyl-2,3-dicyanohydroquinone (PDCHQ, Figure 1a), which, as we showed before, is enzymatically cleaved by the lipase.

The PDCHQ is composed of alkyl chain (14 methylene groups), ester linkage, and head group containing two CN and one OH moiety (Figure 14). One could expect that CN-groups of PDCHQ spread at air/water interface will generate strong SFG signal in the 2200–2300 cm^{-1} frequency region. Indeed, we observed intense band at 2242 cm^{-1} in both infrared and Raman spectra of solid PDCHQ (data not shown). Observation of the same resonance in SFG spectra (Figure 14A) indicates that the PDCHQ molecules adsorb at air/water interface in an ordered form. Because the hydrolysis yields water soluble 2,3-dicyanohydroquinone, the lipase injection into the system should trigger the CN band decay, thus allowing to directly monitor lipase activity by the SFG vibrational spectroscopy.

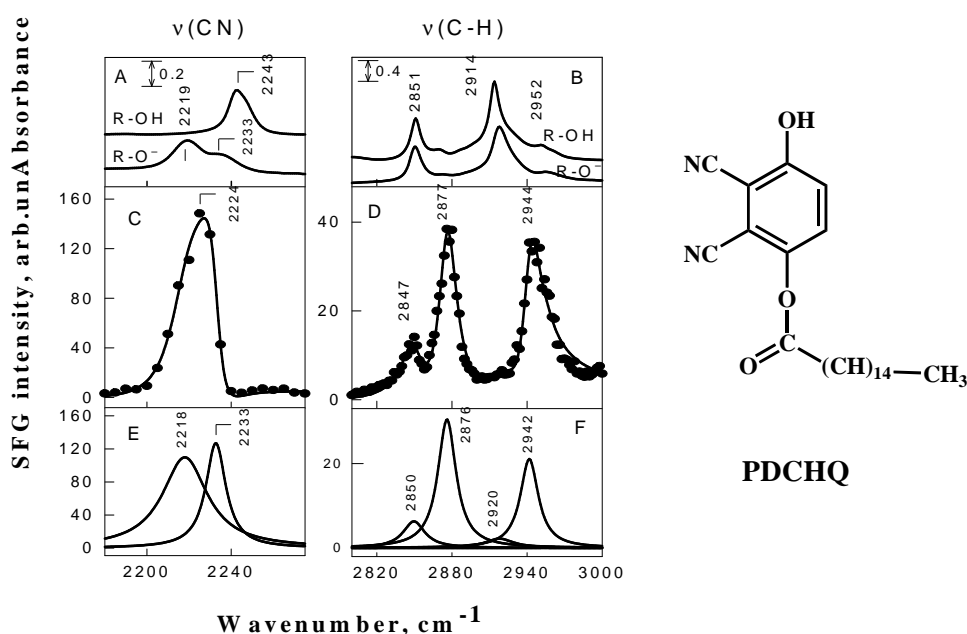


Fig. 14. FT-IR spectra (A, B) of PDCHQ compound in the solid state (R–OH) and in the ionized state in aqueous solution (R–O⁻), and SFG spectra (C, D) of PDCHQ at the air/water interface taken with ssp (s-SFG, s-532 nm, and p-IR) polarization combination. The solid lines (panels C and D) are fits to SFG spectra using Lorentzian functions. Panels E and F show vibrational modes constituting the SFG spectra. The phases of 2218 and 2233 cm^{-1} modes are 0 and π , respectively. The phases of modes in panel F are 0. The solution subphase is 0.1 M NaCl containing 0.01 M NaH_2PO_4 buffer (pH 7.0).

The pronounced peak asymmetry indicates interference effects between several resonances and background. Fitting experimental spectrum reveals the presence of two

resonances located at 2218 and 2233 cm^{-1} (Figure 14B). Interpretation of SFG spectrum requires both experimental (IR and Raman) and theoretical analysis of $\text{C}\equiv\text{N}$ vibrations in PDCHQ and similar compounds. Position of the $\text{C}\equiv\text{N}$ stretching mode provides two-fold information: (i) hydrogen-bonding interaction of CN group at the interface and (ii) ionization state of the OH group. In the solid state, where PDCHQ forms $\text{C}\equiv\text{N}\cdots\text{H}-\text{O}$ hydrogen bonds, FT-Raman and FT-IR spectra show intense *o*-CN peak at 2242 cm^{-1} . It is well known that $\text{C}\equiv\text{N}$ stretching frequency blue shifts upon formation of hydrogen bond due to the reduction of the antibonding character and strengthening of the CN triple bond. Indeed, for PDCHQ dissolved in an aprotic solvent, such as methylene chloride, the $\text{C}\equiv\text{N}$ stretching vibration gives rise to a lower frequency peak at 2238 cm^{-1} . Our SFG spectra suggest that PDCHQ adsorbs at the interface predominantly in the ionized state and the *o*-CN group is hydrogen bonded with water molecules. The involvement of only one of the two CN groups in hydrogen-bonding interaction confirms observation of the different phases for 2233 and 2218 cm^{-1} components (Figure 15 E) denoting that two CN groups point to different directions from the interface. However, we cannot completely discard some residual contribution to the 2233 cm^{-1} component from the $\text{C}\equiv\text{N}$ vibrational mode in neutral PDCHQ molecules. Therefore, we can only safely conclude that the resonance at 2218 cm^{-1} belongs to the hydrogen-bonded *o*-CN group of the PDCHQ oxyanion.

Real time variation of the intensity of $\text{C}\equiv\text{N}$ resonance (2224 cm^{-1}) after the injection of *TLL* into the subphase is demonstrated in Figure 15. Because of relatively low accumulation (60 pulses/point), the time-dependent curves are rather noisy. Without lipase, the $\text{C}\equiv\text{N}$ vibrational signal was found to be relatively stable in the studied time scale. After the addition of WT enzyme, the $\text{C}\equiv\text{N}$ band remains stable for some time and then starts decaying. As seen from Figure 15 (red curves), at some point of time, which is dependent on *TLL* concentration, the decay curve abruptly drops to the background level. Such a steep SF signal decrease might be associated with the collapse of monolayer due to the enzymatic hydrolysis of PDCHQ or/and the strong perturbation of monolayer's order by the enzyme adsorption. To differentiate these effects, we employed the inactivated S146A mutant of *TLL*. As can be seen from Figure 15 a (blue curves), the addition of S146A mutant at 10^{-7} M concentration does not trigger total disappearance of $\text{C}\equiv\text{N}$ resonance. Instead, an approximately 60% drop in signal intensity was detected. These results, we believe, indicate a disruption of ordering of CN dipoles at interface due to the penetration of enzyme into the monolayer. The direct confirmation of lipase penetration into the monolayer and disruption of order could be also obtained from the analysis of the 2800–3750 cm^{-1} and 1500–1800 cm^{-1} frequency range of SFG spectra, which is discussed more thoroughly in dissertation. Here we notice that if the protein-induced disordering exists, it must be sensitive to the enzyme concentration. Figure 16 b shows the time dependence of intensity of the $\text{C}\equiv\text{N}$ resonance after introduction of WT and S146A mutant *TLL* at 10^{-8} M concentration.

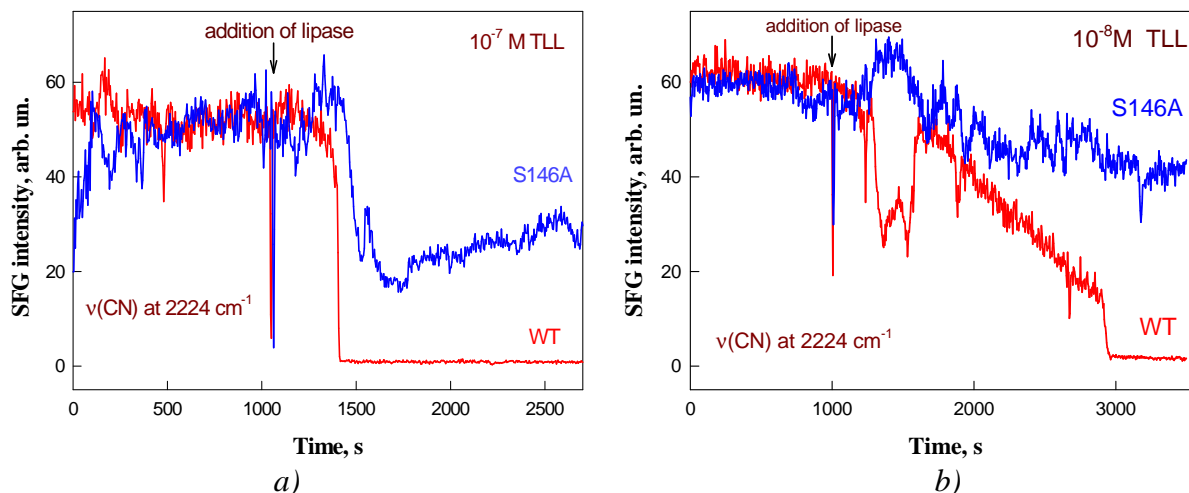


Fig. 15. Time dependence of the intensity of SFG resonance for PDCHQ C≡N stretch at 2224 cm^{-1} after addition WT *TLL* and its S146A mutant of a) 10^{-7} M and b) 10^{-8} concentration.

Reduction of WT enzyme concentration results in two effects: (i) the initial slope of signal decay markedly decreases, and (ii) the time required to fully destroy the CN signal by the WT lipase increases from 400 to 2000 s. On the other hand, the reduction of S146A mutant concentration results in much smaller (of ~20%) decline of C≡N signal. These results prove that enzymatic cleavage indeed takes place at the studied interface. Obvious perturbations of the C≡N mode intensity versus time curve, which starts appearing after 200–600 s after the enzyme injection (Figure 16 b), are presumably due to the adsorption of lipase at interface and interaction with the PDCHQ layer. It is well documented that activity of lipases increases sharply upon binding to the interfaces of lipid aggregates. It should be noted, that while perturbations in 200–600 s interval after the *TLL* (10^{-8} M) injection was observed for all studied samples, these changes were not regular. The most reproducible features in the time-dependent experiments were found to be the time required to decrease the CN signal intensity to zero in the case of WT enzyme, and the residual signal intensity level for the mutant *TLL*. Both parameters depend on the enzyme concentration (Figures 16 a and b) and consequently could be used for the assay of lipase activity. In conclusion, we believe that our work presents a step toward the in situ real-time monitoring of enzymatic processes occurring at air/water interface by the nonlinear sum-frequency generation technique.

CONCLUSIONS

- ∅ The direct electrochemical technique for lipase activity detection was developed using synthetic enzyme substrate containing ferrocene reporting and ester target groups – (9-(5'-ferrocenylpentanoyloxy)nonyl disulfide (FPONDS)); a simple drip-and-dry sensor surface preparation method was suggested.
- ∅ Using SPR and ATR-FT-IR methods we detected the rearrangement of the *Thermomyces lanuginosus* lipase (*TLL*) layer on hydrophobic surfaces, which is followed by a considerable increase of *TLL* activity, thus presenting a direct evidence of the importance of conformational configuration on esterase activity.
- ∅ The utility of the developed electrochemical technique to assess the stereospecificity of esterases, specifically *TLL*, was demonstrated.
- ∅ A rotating disk electrode method was developed, which could be utilized for *TLL* activity detection in micellar substrate systems.
- ∅ The adsorption equilibrium phenomenon between the OPNQ micells and glassy-carbon surface was utilized to develop a *TLL* assay in micellar systems. The technique is based on direct micelle concentration detection, therefore, allows avoiding complications related to the polymorphism of the substrates of esterases.
- ∅ We present sum frequency generation spectroscopy based proof-of-a-concept *TLL* activity assay; the method allows to overcome complications common in classical esterase activity assays related to the polymorphism of substrate, and measures enzyme activity at air/water interface.
- ∅ The tethered bilayer membrane based methodology for the detection of phospholipases by the electrochemical impedance spectroscopy was proposed.

LIST OF PUBLICATIONS

1) **Ignatjev I.**, Valinčius G., Švedaitė I., Gaidamauskas E., Kažemėkaitė M., Razumas V. and Svendsen A.. Direct amperometric determination of lipase activity. *Analytical Biochemistry*, **2005**, Volume 344, Issue 2, p 275-277.

2) Valinčius G., **Ignatjev I.**, Niaura G., Kažemėkaitė M., Talaikytė Z., Razumas V. and Svendsen A.. Electrochemical Method for the Detection of Lipase Activity. *Analytical Chemistry*, **2005**, 77(8): 2632-2636.

3) Niaura G., Kuprionis Z., **Ignatjev I.**, Kažemėkaitė M., Valincius G., Talaikytė Z., Razumas V., and Svendsen A.. Probing of Lipase Activity at Air/Water Interface by Sum-Frequency Generation Spectroscopy. *Journal of Physical Chemistry B*, **2008**, 112, 4094-4101.

4.) Balevičius Z., Vaičikauskas V., Valinčius G. and **Ignatjev I.** Analysis of T. Lanuginosus lipase growth on octadecanethiol using surface Plasmon resonance ellipsometry. *Phys. Stat. Sol.*, **2008**, C. 5, No. 5, 1419-1422.

OTHER COHERENT WITH DISSERTATION PUBLICATIONS

ü Vaičikauskas V., Balevičius Z., **Ignatjev I.** and Valinčius G.. Surface Plasmon Resonance Spectroscopy of Au/ Hexanethiol/ 9-(5'-ferrocenylpentanoyloxy) nonyl disulfide Thin Film. *Lithuanian Journal of Physics*, **2006**, Vol. 46, No. 1, pp. 117-121.

ü Puida M., Ivanauskas F., **Ignatjev I.**, Valinčius G., and Razumas V.. Computational Modelling of the Amperometric Bioanalytical System for Lipase Activity Assay: a Time-Dependent Response. *Noniner Analysis: Modelling and Control*, **2007**, 12, 245-251.

ü Puida M., Ivanauskas F., **Ignatjev I.**, Valinčius G., Razumas V.. Computational modelling of the electrochemical system of lipase activity detection. *Sensors*. **2008**, 8, Iss. 6, 3873-3879.

Conference materials on the subject of dissertation

1.) **Ignatjev I.**, Valinčius G., Švedaitė I., Gaidamauskas E.. *Naujas elektrocheminis metodas lipazės aktyvumo nustatymui*, "Chemija 2005", p. 48–49, **2005**.

2.) **Ignatjev I.**, Milkantaitė D., Razumas V., Kažemėkaitė M., Valinčius G.. 2-oksipalmitoil–1,4–naftochinono ir tritono X-100 micelinės sistemos naudojimas fermento aktyvumui nustatyti, "Chemija ir cheminė technologija 2007", p.96-100, **2007**.

3.) **Ignatjev I.**, Milkantaitė D., Balevičius Z., *Redox-active Physisorbed Monolayers: Substrates for Electrochemical Lipase Activity Assay*, Nanoscale Engineering of the Biointerface, Playa del Aro, Spain (28 May–1 June) **2007**

INTERNSHIP

From 2006–01–22 to 2006–03–23 – Carnegie Mellon University, JAV.

ACKNOWLEDGMENTS

Heartily thank:

to my scientific supervisor dr. doc. Gintaras Valinčius for giving me the opportunity to become involved in the research and the thorough support on the dissertation, for his kindness;

to acad. of LAS, prof. habil. dr. Valdemaras Razumas head of department of Bioelectrochemistry and Biospectroscopy for advice, support on discussions, facility work with good stuff and competitive co-workers;

to habil. dr. Gediminas Niaura bei dr. Zita Talaikytė for help performing various spectroscopic measurements and discussions

to dr. Marytė Kažemėkaitė and dr. Irena Švedaitė for substrates synthesis which were used for in this work for detection of enzyme activity;

to dr. Allan Svendsen, from Novozymes company, head of science investigation department, for free sent to us mutant of TLL;

to dr. Zenonas Kuprionis employee in „EKSPLA“ company for providing to work with SFG spectroscope;

to dr. Viktoras Vaičiškauskas and dr. Zigmui Balevičiui from institute of Physic for collaboration in the field of surface plasmon resonance spectroscopy;

to prof. habil. dr. Feliksas Ivanauskas and his graduate students Mantas Puida from Vilnius University MIF for development of mathematic models and their employment for our analyzed system;

to dr. David Vanderah from NIST'o (Institute of National Standards and Technologies, Maryland, JAV), for synthesized analoge of phosphoroline – WC14 and Frank Heinrich (NIST, Maryland, JAV) for covered with magnetron Si wafers Au and for sending them to Lithuania;

to all colleagues at Bioelectrochemistry and Biospectroscopy department for there cooperation and contribution;

to the Lithuanian State Science and Studies Foundation for financial support;

to my darling family for their unlimited support, patience and understanding.

Santrauka

Pasiūlytas tiesioginis lipazės aktyvumo detekcijos metodas, panaudojant sintetinį fizisorbuotą substratą, 9-(5'-ferocenilpentanoiloksi)nonildisulfidą (FPONDS), turintį feroceno redokso žymę ir esterinę fermento taikinio grupę. Metodas pasižymi paprasta „drip-and-dry“ sensorinio paviršiaus paruošimo technologija. PPR ir ATR-FT-IR metodais stebėtas *Thermomyces lanuginosus* lipazės (*TLL*) sluoksnio persitvarkymas ant hidrofobinio paviršiaus, kurį lydi žymus *TLL* aktyvumo augimas, kai substratu naudojamas FPONDS, o tai įrodo konformacinių pokyčių svarbą fermento aktyvumui. Pademonstruota galimybė siūlomą elektrocheminį metodą panaudoti esterazių, pavyzdžiui *TLL* stereospecifiškumui įvertinti. Pasiūlytas sukamojo diskinio elektrodo metodas, leidžiantis detektuoti *TLL* aktyvumą micelių substratų sistemose. Absorbcinės pusiausvyros reiškinys tarp OPNQ micelių tirpale ir stiklo grafitinio elektrodo panaudotas *TLL* aktyvumui nustatyti micelių sistemose. Metodas grindžiamas tiesioginiu micelių koncentracijos nustatymu, todėl sumažėja esterazių substrato polimorfizmo įtaka analizei. *TLL* pavyzdžiu pasiūlyta esterazių aktyvumo detekcijos koncepcija, besiremianti suminio dažnio generacijos spektroskopijos metodu taikymu fazių sąlyčio riboje oras/vanduo; metodas leidžia išvengti komplikacijų, susijusių su substratų polimorfizmu, būdingų klasikiniams esterazių aktyvumo nustatymo metodams. Pasiūlytas elektrocheminio impedanso spektroskopinis metodas fosfolipazių aktyvumui detektuoti, panaudojant prijungtas prie paviršiaus bisluoksnės membranas.

CURRICULUM VITAE

Surname, name:	Ilja Ignatjev
Birth date and place:	1980 09 23 Pskov, Russia
e-mail	ilja@bchi.lt
Education:	
1998	Graduation certificate of secondary school.
1998–2002	Bachelor of Science (in Chemistry) Vilnius University, Lithuania.
2002–2004	Magister of Science (in Chemistry) Vilnius University and Institute of Biochemistry, Lithuania,
2004–2008	Department of Bioelectrochemical and biospectroscopic, Biochemistry Institute. Doctoral studies, Lithuania.